

Linear response theory

8.512 Theory of solids II (Spring 2022)

Topics:

- The general theory for representing measurable quantities by correlation functions (the Kubo and fluctuation-dissipation theorems, the arrow of time, causality and sum rules);
- Dynamical compressibility and collective modes in interacting electron systems
- Magnetism I: ferro- and antiferromagnetic long-range order
- Magnetism II: Stoner instability, quantum-Hall “ferromagnetic states,” spontaneous valley and spin polarization in moiré graphene
- Neutron and x-ray scattering
- Peierls instability, Kohn anomaly and charge density waves
- Landau Fermi-liquid theory
- Plasmon excitations in 3D and 2D;
- Linear response in superconductors.

Measurements and Correlation Functions

- Experiments probe non-equilibrium properties.
- In physical measurements we drive the system out of equilibrium, create an excitation (disturbance), and measure some observable
- Non-equilibrium quantities: dynamical compressibility, conductivity, scattering cross-section, etc.
- Theoretical picture is best developed for the equilibrium state
- Fortunately, the Kubo formula and the fluctuation-dissipation theorem link the two.
- Can understand response functions to weak applied fields entirely from knowledge of equilibrium properties

This is a big deal! (details in “Measurements and correlation functions” by P Martin)

Weak probes and Kubo susceptibility

- The magic of the linear response: probing the system in its ground state through a non-equilibrium process
- The notion of linear susceptibility χ_{ji} : response of an observable O_j to the perturbation O_i
- System Hamiltonian $\mathcal{H} = \mathcal{H}_0 + O_i f_i(t)$;
Susceptibility

$$\chi_{ji} = \frac{\text{"response"} }{\text{"force"} f_i}, \quad \langle O_j(t) \rangle = \int_{-\infty}^{\infty} dt' \chi_{ji}(t-t') f_i(t')$$

- Relate χ_{ji} to the properties of the system in equilibrium:

$$\chi_{ji}(t - t') = \frac{i}{\hbar} \Theta(t - t') \langle G | [O_j(t), O_i(t')] | G \rangle$$

- At $T > 0$ replace $\langle G | \dots | G \rangle \rightarrow \frac{1}{Z} \sum_{\alpha} e^{-\beta E_{\alpha}} \langle \alpha | \dots | \alpha \rangle$

Examples

Perturb system by driving it out of equilibrium, then measure an observable O_i . E.g. particle density (**compressibility**), current (**conductivity**), or magnetization (χ_{spin}):

System Hamiltonian with a perturbation describing a weak probe.

$$\mathcal{H} = \mathcal{H}_0 + \mathcal{H}'(t), \quad \mathcal{H}'(t) = \sum_j O_j A_j(t)$$

E.g. for O_i being particle density:

$$\mathcal{H}' = \int \hat{\rho}(x, t) U(x, t) d^3x$$

with $\hat{\rho}(x, t) = \sum_i \delta(x - x_i(t))$ in 1st quantization and $\hat{\rho}(x, t) = \psi^\dagger(x)\psi(x)$ in 2nd quantization. Or, a magnetic coupling

$$\mathcal{H}' = - \int \hat{m}_z(x, t) H_z(x, t) d^3x, \quad \hat{m}_z = \mu(\hat{\rho}_\uparrow - \hat{\rho}_\downarrow)$$

Or, electric current coupled to the EM vector potential

$$\mathcal{H}' = - \int \frac{1}{c} \mathbf{j}(x, t) \mathbf{A}(x, t) d^3x, \quad \mathbf{E} = - \frac{1}{c} \partial \mathbf{A} / \partial t$$

Linear response theory: derive the Kubo formula

A system driven out of equilibrium, $H = H_0 + H'$, $H' = \sum_i O_i A_i(t)$,

$$\langle O_j(t) \rangle_{n.e.} = \langle O_j(t) \rangle + \int d\tau \chi_{ji}(t - \tau) A_i((\tau) + \dots) \quad (1)$$

Steps to derive the response function χ_{ji} : 1) Express χ_{ji} through the thermal equilibrium state in distant past $A_j(\tau) \rightarrow 0$ as $\tau \rightarrow -\infty$:

$$\langle O_j(t) \rangle_{n.e.} = Z_0^{-1} \sum_{\alpha} e^{-\beta \epsilon_{\alpha}} \langle \alpha | U^{\dagger}(-\infty, t) O_j U(-\infty, t) | \alpha \rangle, \quad Z_0 = \text{Tr} e^{-\beta H_0}$$

2) Express the evolution operator as time-ordered power series

$$U(t_0, t) = U_0(t - t_0) \times \text{Texp} \left(-i \int_{t_0}^t dt' H'_I(t') \right). \quad \text{Here we are working in}$$

the "interaction representation" $H'_I = U_0^{\dagger}(t - t_0) H' U_0(t - t_0)$,

$$U_0(t - t_0) = \exp(-iH_0 t / \hbar). \quad (\text{the choice of the initial time } t_0 \text{ is completely arbitrary})$$

$$3) \text{ Next, expand in } H'_I \text{ as } U(t_0, t) = U_0(t - t_0) \left[1 - i \int_{t_0}^t dt' H'_I(t') + \dots \right].$$

At 1st order in H'_I this gives (a result independent of the time t_0)

$$\chi_{ji}(t - t') = \Theta(t - t') \frac{i}{\hbar} \langle [O_j(t), O_i(t')] \rangle \quad (2)$$

The Heaviside function is a direct consequence of **causality** – that is, an applied field can impact **the future dynamics but not the past dynamics**.

Fourier representation of susceptibility

Since the unperturbed Hamiltonian is time-independent it is clear that the linear response is diagonal in frequency. Namely, if the system is perturbed at a frequency ω , the linear response will be at frequency ω as well:

$$\langle O_j(\omega) \rangle = \sum_i \chi_{ji}(\omega) A_i(\omega)$$

where $\langle O_j(\omega) \rangle$, $\chi_{ji}(\omega)$ and $A_i(\omega)$ are the Fourier transforms of $\langle O_j(t) \rangle$, $\chi_{ji}(t)$ and $A_i(t)$:

$$A_i(\omega) = \int_{-\infty}^{\infty} e^{i\omega t} A_i(t) dt, \quad \chi_{ji}(\omega) = \int_{-\infty}^{\infty} e^{i\omega t} \chi_{ji}(t) dt$$

- ☺: Mathematically speaking, this is perfectly natural since under FT a convolution in Eq.(1) turns into a product.
- ☺: We will use both positive and negative frequencies!
- ☺: Since $f(\omega) = f^*(-\omega)$ for FT of a real-valued function, the real and imaginary parts of $\chi_{ji}(\omega) = \chi'_{ji}(\omega) + i\chi''_{ji}(\omega)$ are even and odd in ω , respectively.

The arrow of time and Fourier transform

Because of causality, $\chi(\tau < 0) = 0$ in Eq.(1). The Fourier transform

$$\chi_{ij}(z) = \int_{-\infty}^{\infty} dt e^{izt} \chi_{ij}(t) = \int_0^{\infty} dt e^{izt} \chi_{ij}(t)$$

is therefore analytic in the upper half plane of complex frequency,
 $\text{Im } z > 0$. This analyticity property is a **nontrivial, but extremely useful** mathematical consequence of the arrow of time.

Many constraints on the ω dependence, both the obvious ones and the surprising ones.

To illustrate the connection between causality and the analytic properties under Fourier transform consider $\chi(t) = \Theta(t)Ae^{-\gamma t}$. This is a memory function with the memory loss rate $\gamma > 0$.

In this case we have $O_j(t) = \int_{-\infty}^t dt' Ae^{-\gamma(t-t')} f_i(t')$. The Fourier transform

$$\chi(z) = \int_0^{\infty} dt A e^{izt - \gamma t} = \frac{A}{\gamma - iz}. \quad (3)$$

This expression has a pole at $z = -i\gamma$ in the lower halfplane $\text{Im } z < 0$, and is analytic at $\text{Im } z > 0$.

Analytic functions? See excellent [18.04 notes](#), or a summary at the end

Sanity check: harmonic oscillator susceptibility

Hamiltonian $H = \frac{p^2}{2m} + \frac{m\omega_0^2}{2}x^2 - exE(t)$. Find Kubo polarizability?

Dipole moment $d = (O_j) = ex$, the “force” E couples to $O_i = -d$.

Dynamic polarizability, defined as $\langle d(t) \rangle = \int_{-\infty}^t \chi(t-t')E(t')dt'$, equals

$$\chi_{Kubo}(t-t') = -\frac{i}{\hbar} \langle G | [d(t), d(t')] | G \rangle$$

Quantum harmonic oscillator evolution is identical to the classical one.

Therefore $x(t) = x(t') \cos \omega_0(t-t') + \frac{p(t')}{m\omega_0} \sin \omega_0(t-t')$. Plugging it in the Kubo formula and combining with the equal-time commutators $[x(t'), x(t')] = 0$, $[x(t'), p(t')] = i\hbar$ gives a result (!!!) identical to the classical oscillator polarizability response

$$\chi_{Kubo}(t-t') = -\frac{ie^2}{\hbar} i\hbar \frac{1}{m\omega_0} \sin \omega_0(t-t') = \frac{e^2}{m\omega_0} \sin \omega_0(t-t')$$

Fourier transform (infinitesimal damping η added to control convergence)

$$\begin{aligned} \chi(\omega) &= \int_0^\infty dt e^{i\omega t - \eta t} \chi(t) = \frac{e^2}{2im\omega_0} \left(\frac{1}{\eta - i(\omega + \omega_0)} - \frac{1}{\eta - i(\omega - \omega_0)} \right) \\ &= \frac{e^2}{m(\omega_0^2 - (\omega + i\eta)^2)}, \quad \text{complex poles : } \omega_{1,2} = \pm\omega_0 - i\eta, \quad \text{Im } \omega_{1,2} < 0 \end{aligned}$$

The poles $\omega_{1,2}$ reside in the lower halfplane of complex ω . This agrees

with analyticity and matches the response of a damped classical

Symmetry properties of susceptibility

Since O_j are Hermitian operators, it follows that (check!)

$$\chi_{ji}(\omega) = -\chi_{ij}(-\omega) = -[\chi_{ji}(-\omega)]^* = [\chi_{ij}(\omega)]^*$$

is a Hermitian matrix. Decomposing into a sum of the real and imaginary parts

$$\chi_{ji}(\omega) = \chi'_{ji}(\omega) + i\chi''_{ji}(\omega)$$

and setting $j = i$ we see that $\chi''_{jj}(\omega)$ is real and an odd function of ω .

Likewise, $\chi'_{jj}(\omega)$ is a real, even function of ω .

Other symmetry properties of χ_{ji} can be derived from symmetries of H . For instance, if H is time-reversal invariant, and if $f_i(t) \rightarrow \epsilon_i f_i(-t)$ under time-reversal, then it is easy to see that

$$\chi_{ji}(\omega) = -\epsilon_i \epsilon_j \chi_{ij}(-\omega) = \epsilon_i \epsilon_j \chi_{ji}(\omega)$$

The reason we need to include the “signature,” ϵ_i , is that some operators that we are interested in, such as a position or an electric potential, are even under time-reversal, $\epsilon_i = 1$, while others, such as the current or the magnetic field, are odd, $\epsilon_i = -1$.

Identification of $\chi''_{ij}(\omega)$ with dissipation

Consider the rate at which power is absorbed from a generic external field

$$\begin{aligned} P(t) &= \frac{d\langle H \rangle}{dt} = \sum_j \frac{\partial \langle H \rangle}{\partial A_j} \dot{A}_j = \sum_j \langle O_j(t) \rangle_{n.e.} \dot{A}_j \\ &= \int d\tau \chi_{ji}(\tau) A_i(t - \tau) \dot{A}_j(t) = \iint \frac{d\omega d\nu}{(2\pi)^2} e^{i(\omega - \nu)t} \chi_{ji}(\omega) A_i(\omega) i\nu A_j(-\nu) \end{aligned}$$

Typically, we are not interested in the rapidly oscillating pieces of P but only in its time average. We thus integrate over t [to enforce approximate δ -function in frequency through $\int dt e^{i(\omega - \nu)t} = 2\pi\delta(\omega - \nu)$]:

$$\int dt P(t) = \int \frac{d\nu}{2\pi} \chi_{ji}(\nu) A_i(\nu) i\nu A_j(-\nu)$$

Since $A_j(t)$ is real, $A_j(-\omega) = A_j^*(\omega)$. Using $\chi_{ji}(-\nu) = \chi_{ji}^*(\nu)$ we have

$$\int dt P(t) = \int \frac{d\nu}{2\pi} \nu \chi''_{ji}(\nu) A_i(\nu) A_j^*(\nu)$$

Since dissipated power is always positive (2nd law of thermodynamics), it follows that $\nu \chi''_{ii}(\nu) \geq 0$. (Which agrees with the symmetry properties, see above)

This result checks with the harmonic oscillator response found above:

$$\chi''(\omega) \sim \delta(\omega - \omega_0) - \delta(\omega + \omega_0)) \text{ (odd in } \omega \text{ and positive for } \omega > 0\text{)}$$

Interacting electrons in metals

Dynamical compressibility and collective modes in interacting electron systems

Topics:

- The dielectric function and dynamical screening
- Polarization susceptibility (the Lindhard function)
- Collective charge oscillations (plasma waves)
- Collective phase modes in superconductors (the Anderson-Higgs phenomenon)
- Friedel oscillations, Kohn anomaly and Peierls instability

The polarization response and the dielectric function

We will start with considering the electron density response to a potential $U_{\text{ext}}(\mathbf{q}, \omega) \sim e^{i\mathbf{q}\mathbf{x} - i\omega t}$. This response is described by polarization susceptibility defined as a density-potential response $\delta n = \chi(\mathbf{q}, \omega) U_{\text{ext}}$,

$$\chi(\mathbf{q}, \omega) = \frac{i}{\hbar} \int_0^\infty \langle 0 | [n_q(t), n_{-\mathbf{q}}(0)] | 0 \rangle e^{i\omega t} dt$$

with the density harmonics $n_q(t) = \int d^3x e^{-i\mathbf{q}\mathbf{x}} \delta n(\mathbf{x}, t)$. The quantity $\chi(\mathbf{q}, \omega)$ will now be shown to be related to the dielectric function as

$$\epsilon(\mathbf{q}, \omega) = 1 - \frac{4\pi e^2}{\mathbf{q}^2} \chi(\mathbf{q}, \omega) \quad (4)$$

(in cgs units). To derive Eq.(4) recall the dielectric screening (the quasielectrostatic approximation, or "finite- ω " electrostatics):

$$\frac{1}{\epsilon(\mathbf{q}, \omega)} = \frac{U_{\text{tot}}(\mathbf{q}, \omega)}{U_{\text{ext}}(\mathbf{q}, \omega)} = 1 + \frac{U_{\text{ind}}(\mathbf{q}, \omega)}{U_{\text{ext}}(\mathbf{q}, \omega)} \quad (\text{Why so?})$$

The induced potential is related to the induced charge density through Poisson's equation $-\nabla^2 U_{\text{ind}} = 4\pi e^2 \delta n_{\text{ind}}$, i.e. $U_{\text{ind}}(\mathbf{q}, \omega) = \frac{4\pi e^2}{\mathbf{q}^2} \delta n_{\text{ind}}$.

Substituting $\delta n_{\text{ind}} = \chi(\mathbf{q}, \omega) U_{\text{tot}} = \chi(\mathbf{q}, \omega) \frac{U_{\text{ext}}}{\epsilon(\mathbf{q}, \omega)}$ and solving for $\epsilon(\mathbf{q}, \omega)$ gives Eq.(4).

Beware of notation: In many-body literature the polarization susceptibility is denoted $\Pi(\mathbf{q}, \omega)$ (and is called **polarization function**). Except for the next two pages we will be using Π instead of χ .

Compare to electrostatics

Connect microscopic polarizability to the properties of the dielectric screening function $\epsilon(q)$.

Polarization in electrostatics: $D = \epsilon E$, $\nabla \cdot D = 4\pi\rho_{\text{ext}}$, $\nabla \cdot E = 4\pi\rho_{\text{tot}}$. Then, we have $eD = -\nabla U_{\text{ext}}$ and $eE = -\nabla U_{\text{tot}}$. Assuming linear response,

$$\nabla \cdot E = 4\pi\rho_{\text{tot}} = 4\pi(\rho_{\text{ext}} + \rho_{\text{ind}})$$

giving $-\nabla^2 U = 4\pi e(\rho_{\text{ext}} + \rho_{\text{ind}})$, where $U \equiv U_{\text{tot}}$. After Fourier transform

$$q^2 U(q) = 4\pi e(\rho_{\text{ext}}(q) + \rho_{\text{ind}}(q))$$

Combine it with a microscopic relation $\rho_{\text{ind}}(q) = e\chi(q)U(q)$ to obtain $U(q) = U_{\text{ext}}(q) + \frac{4\pi e^2}{q^2}\chi(q)U(q)$. This gives

$$U(q) = U_{\text{ext}}(q)/(1 - \frac{4\pi e^2}{q^2}\chi(q))$$

Therefore, $\epsilon(q) = 1 - \frac{4\pi e^2}{q^2}\chi(q)$. This relation remains unchanged for the dynamic screening so long as we can ignore the retardation due to the finite speed of light. "Finite- ω " electrostatics!

The static and dynamic (long-wavelength) screening

a) $\omega = 0$, q finite; In this case the mean-field Thomas-Fermi screening approximation is a simplest microscopic model:

$$n(x) = n(\epsilon_F(x)) = n_0 - \frac{\partial n}{\partial \mu} U(x), \text{ valid for } |q| \ll k_F. \text{ Thus}$$

$\chi(k \rightarrow 0)_{\omega=0} = -\frac{\partial n}{\partial \mu}$. The quantity $\frac{\partial n}{\partial \mu}$ is called *compressibility*. For a free-electron gas, $\frac{\partial n}{\partial \mu} = 2N(0)$. Hence, $\frac{1}{\epsilon(q)} = \frac{q^2}{q^2 + (4\pi e^2 \frac{\partial n}{\partial \mu})} = \frac{q^2}{q^2 + \kappa_{TF}^2}$.

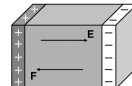
The screened potential of a point charge is of the form

$$U(x) = \sum_q e^{-iqx} \frac{4\pi e^2}{q^2 \epsilon(q)} = \sum_q e^{-iqx} \frac{4\pi e^2}{q^2 + \kappa_{TF}^2} = \frac{e^2}{|x|} e^{-\kappa_{TF}|x|}.$$

b) ω finite, $q \rightarrow 0$ (the long-wavelength limit, classical EM!). In this case, a simple classical free-electron model for $\epsilon(\omega)_{q=0}$ gives the dynamic screening function

$$\epsilon(\omega) = 1 - \frac{\omega_p^2}{\omega^2 + i\omega\gamma}, \quad \omega_p^2 = \frac{4\pi e^2 n}{m}$$

This corresponds to $\chi(q, \omega) = \frac{nq^2}{m(\omega^2 + i\omega\gamma)}$. Collective charge oscillations



with plasma frequency ω_p (for weak damping γ).

Next, we reproduce and generalize these results microscopically.

This page intentionally left blank

Express $\chi_{ji}(\omega)$ through microscopic quantities

Use the eigenstates of H_0 , $\epsilon_\alpha |\alpha\rangle = H_0 |\alpha\rangle$, and identity decomposition $1 = \sum_\alpha |\alpha\rangle\langle\alpha|$ to bring $\chi_{ji}(\omega) = \int dt e^{i\omega t} \frac{i}{\hbar} \langle [O_j(t), O_i(0)] \rangle$ to the form

$$\begin{aligned}\chi_{ji}(\omega) &= \frac{i}{\hbar Z_0} \sum_{\alpha\beta} e^{-\beta\epsilon_\alpha} \langle \alpha | O_j | \beta \rangle \langle \beta | O_i | \alpha \rangle \int_0^\infty e^{i(\epsilon_\alpha - \epsilon_\beta)t} e^{i\omega t} e^{-\delta t} dt \\ &\quad - \frac{i}{\hbar Z_0} \sum_{\alpha\beta} e^{-\beta\epsilon_\beta} \langle \beta | O_j | \alpha \rangle \langle \alpha | O_i | \beta \rangle \int_0^\infty e^{i(\epsilon_\alpha - \epsilon_\beta)t} e^{i\omega t} e^{-\delta t} dt \\ &= \frac{1}{Z_0} \sum_{\alpha\beta} \langle \beta | O_j | \alpha \rangle \langle \alpha | O_i | \beta \rangle \frac{e^{-\beta\epsilon_\beta} - e^{-\beta\epsilon_\alpha}}{\omega - (\epsilon_\beta - \epsilon_\alpha) + i\delta} \end{aligned} \tag{5}$$

We swapped α and β in 2nd term, and added a factor $e^{-\delta t}$ to assure convergence.

This result is completely general (no approximations made!). We will use it later to derive the fluctuation-dissipation theorem and sum rules.

Eq.(5) is an explicit expression that would be useful if we knew the many-body eigenstates and the respective matrix elements. Below, as an illustration, we use it to derive dynamic compressibility of a fermi gas.

Polarization response of free fermions from Kubo theory

We consider susceptibility defined as a density-potential response $\delta n = \Pi(\mathbf{q}, \omega)U$, where U is the true microscopic potential (which includes screening) and $\Pi(\mathbf{q}, \omega) = \frac{i}{\hbar} \int_0^\infty \langle 0 | [n_{\mathbf{q}}(t), n_{-\mathbf{q}}(0)] | 0 \rangle e^{i\omega t} dt$. In general, $\Pi(\mathbf{q}, \omega) = \sum_{\alpha} \frac{|\langle \alpha | n_{\mathbf{q}}^\dagger | 0 \rangle|^2}{\omega - (E_{\alpha} - E_0) + i\eta} - \frac{|\langle \alpha | n_{-\mathbf{q}}^\dagger | 0 \rangle|^2}{\omega + (E_{\alpha} - E_0) + i\eta}$. The quantity $\Pi(\mathbf{q}, \omega)$ is called *polarization function*.

For free fermions $n_{\mathbf{q}}^\dagger = \sum_{\mathbf{k}} c_{\mathbf{k}+\mathbf{q}}^\dagger c_{\mathbf{k}}$. So, the excited state $|\alpha\rangle$ describes $|\text{hole at } \mathbf{k}, \text{ electron at } \mathbf{k} + \mathbf{q}\rangle$. Hence, $|\langle \alpha | n_{\mathbf{q}}^\dagger | 0 \rangle|^2 = (1 - f_{\mathbf{k}+\mathbf{q}})f_{\mathbf{k}}$, and

$$\Pi(\mathbf{q}, \omega) = \sum_{\mathbf{k}} \frac{(1 - f_{\mathbf{k}+\mathbf{q}})f_{\mathbf{k}}}{\omega - (\epsilon_{\mathbf{k}+\mathbf{q}} - \epsilon_{\mathbf{k}}) + i\eta} - \frac{(1 - f_{\mathbf{k}-\mathbf{q}})f_{\mathbf{k}}}{\omega - (\epsilon_{\mathbf{k}-\mathbf{q}} - \epsilon_{\mathbf{k}}) + i\eta}$$

The ff terms cancel after shifting momenta in the second term, giving

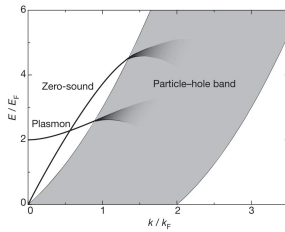
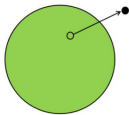
$$\Pi(\mathbf{q}, \omega) = \sum_{\mathbf{k}} \frac{f_{\mathbf{k}} - f_{\mathbf{k}+\mathbf{q}}}{\omega - (\epsilon_{\mathbf{k}+\mathbf{q}} - \epsilon_{\mathbf{k}}) + i\eta}$$

This quantity—the free-fermion $\Pi(\mathbf{q}, \omega)$ —is known as *the Lindhard function*.

Particle-hole excitations

The continuum of particle-hole excitations

$\text{Im}\Pi(\mathbf{q}, \omega) = \sum_k (f_k - f_{k+\mathbf{q}})\delta(\omega - \epsilon_{k+\mathbf{q}} + \epsilon_k)$ —governs damping and absorption.



Response of a free Fermi gas: agreement with simple models. Static limit, Thomas-Fermi screening

Polarization function in the static limit? $\Pi(q \rightarrow 0)_{\omega=0} = \sum_k \frac{f_k - f_{k+q}}{\epsilon_k - \epsilon_{k+q}}|_{q \rightarrow 0}$
 $= \sum_k \frac{\partial f_k}{\partial \epsilon_k} \approx - \sum_k \delta(\epsilon_k - \mu) = - \frac{\partial n}{\partial \mu}$ where we approximated

$\frac{\partial f_k}{\partial \epsilon_k} = -\beta f_k(1 - f_k) \approx -\delta(\epsilon_k - \mu)$ (we assume $kT \ll \mu$). This links

$\Pi_{\omega=0}$ with the static compressibility, $\Pi(q \rightarrow 0) = -\frac{\partial n}{\partial \mu}$, giving the dielectric function with a strong q dependence

$$\epsilon(q \rightarrow 0)_{\omega=0} = 1 + \frac{4\pi e^2}{q^2} \frac{\partial n}{\partial \mu} = 1 + \frac{\kappa_{TF}^2}{q^2}, \text{ where } \kappa_{TF}^2 = 4\pi e^2 \frac{\partial n}{\partial \mu}.$$

Therefore, the **screened Coulomb potential** is $V(q) = \frac{4\pi e^2}{\epsilon(q)q^2} = \frac{4\pi e^2}{q^2 + \kappa_{TF}^2}$.

Inverse Fourier transform gives a simple dependence $V(x) = \frac{e^2}{|x|} e^{-\kappa_{TF}|x|}$.

Here is a less dry derivation. Potential of a point charge satisfies

Poisson's equation $-\nabla^2 V(x) = 4\pi e^2 \left(\delta(x) - \frac{\partial n}{\partial \mu} V(x) \right)$, where the last term is the Thomas-Fermi mean-field "self-induced" charge polarization. This equation can be easily solved in direct space or by

Fourier-transforming to $V(q) = \frac{4\pi e^2}{q^2 + \kappa_{TF}^2}$ and $V(x) = \frac{e^2}{|x|} e^{-\kappa_{TF}|x|}$ as above.

The Thomas-Fermi model gives a coarse-grained description of screening which ignores the high- q harmonics with $|q| \sim k_F$. To be refined later!

Response of a free Fermi gas: agreement with simple models. Dynamic response, high frequencies

Polarization function at high frequencies $\omega \gg qv_F$ and long wavelengths $q \ll 2k_F$?

$$\begin{aligned}\Pi(q, \omega)_{qv_F \ll \omega} &= \sum_k \frac{(f_k - f_{k+q})(\epsilon_{k+q} - \epsilon_k)}{\omega^2} = -\frac{2}{\omega^2} \int \frac{d^3 k}{(2\pi)^3} (q\nabla_k) f_k (q\nabla_k) \epsilon_k \\ &= \frac{2}{\omega^2} \int \frac{d^3 k}{(2\pi)^3} f_k (q\nabla_k)^2 \epsilon_k = \frac{2}{\omega^2} \int \frac{d^3 k}{(2\pi)^3} f_k \frac{q^2}{m} = \frac{nq^2}{m\omega^2}\end{aligned}$$

This gives the dielectric function $\epsilon(\omega) = 1 - \frac{4\pi e^2}{q^2} \frac{nq^2}{m\omega^2} = 1 - \frac{\omega_p^2}{\omega^2}$, as expected. For a good metal, the **plasma frequency** values

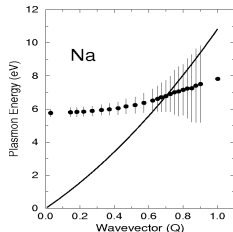
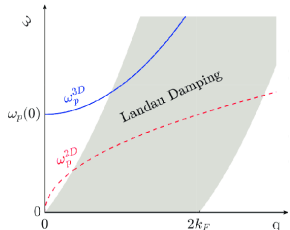
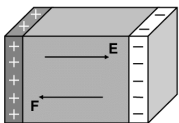
$\omega_p = \left(\frac{4\pi n e^2}{m} \right)^{1/2}$ lie in the UV part of optical spectrum. E.g. in Copper $n = 8.5 \cdot 10^{22} \text{ cm}^{-3}$, $\omega_p = 1.64 \cdot 10^{16} \text{ s}^{-1} = 2.61 \cdot 10^{15} 2\pi \text{ Hz} \approx 10.8 \text{ eV}$.

Collective modes are described by the poles of $\epsilon(\omega)$. Indeed, the relation $\epsilon(\omega)U_{\text{tot}} = U_{\text{ind}}$ implies that if ω satisfies $\epsilon = 0$, charge polarization will have an oscillatory dynamics even in the absence of U_{ind} . These are the collective **plasma oscillations** (more on that below).

Collective plasma oscillations

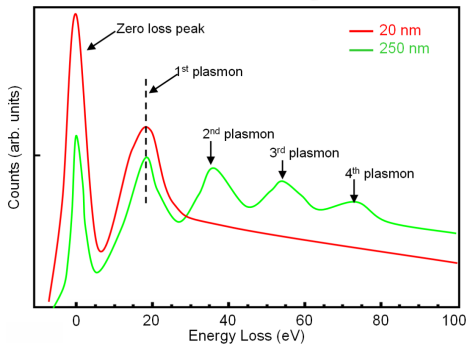
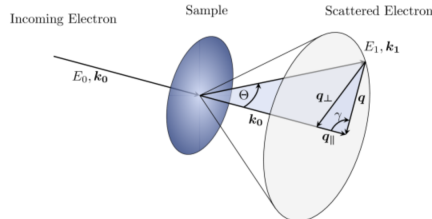
Collective plasma oscillations, plasmon modes

Collective excitations in solids in which many electrons move together synchronized by long-range Coulomb forces. Wide interest in plasmons stems from their hybrid charge-field character, a property that makes these excitations central to the research at the frontier of electronics and photonics.



Plasmon modes are described by zeroes of $\epsilon(q, \omega)$. Indeed, the relation $\epsilon(q, \omega)U_{\text{tot}} = U_{\text{ind}}$ implies that, so long as ω satisfies $\epsilon(q, \omega) = 0$, the collective charge oscillations occur even in the absence of U_{ind} . Plasmon oscillations are undamped if ω , for a given q , lies outside the particle-hole continuum. Plasmon mode dispersion has a different form for different space dimensionality. It is gapped in 3D and gapless in 2D and 1D.

Plasmons from electron energy loss spectroscopy in thin silicon films



Plasmon mode dispersion at small q

Weak dispersion in 3D. From $\epsilon(q, \omega) = 1 - \frac{4\pi e^2}{q^2} \Pi(q, \omega) = 0$, we expand $\Pi(q, \omega)$ to next order in $qv_F/\omega \ll 1$:

$$\Pi(q, \omega) = \frac{nq^2}{m\omega^2} \left(1 + A \frac{q^2 v_F^2}{\omega^2} + \dots\right)$$

Substituting in $\epsilon(q, \omega)$, we obtain the dispersion relation at small q :

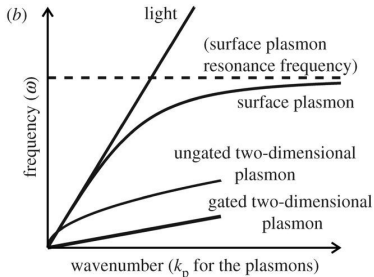
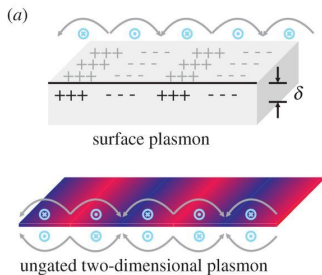
$$\omega^2 = \omega_p^2 + A q^2 v_F^2 + O(q^4)$$

The mode is undamped at small q . At higher q it plunges into the particle-hole continuum and becomes Landau-damped ($p \rightarrow e-h$ pairs).

Plasma oscillations of 2D electrons have a very different character than 3D plasmons. This is so because the $1/r$ electric fields, by which charges in 2D interact, live in the 3D outer space, and thus are not screened by the 2D charge dynamics. Plasma oscillations are still described by $\epsilon(q, \omega) = 1 - V(q)\Pi(q, \omega) = 0$, with $V(q)$ the 2D Fourier transform of the 3D Coulomb potential $\int d^2 r \frac{e^2}{r} e^{-iqr} = \frac{2\pi e^2}{q}$. Taking $\Pi(q, \omega) = \frac{nq^2}{m\omega^2}$ gives plasmon modes with a **strong square-root dispersion** $\omega \sim \sqrt{q}$.

Surface plasmons

Large wavenumbers $q \gg \omega/c$, short wavelengths. Strong field confinement out of plane: $V(r) \sim e^{iq_x x + q_y y} e^{-|q|z}$, $z > 0$. In graphene, confinement lengthscales $\xi = 1/q \sim 0.2\mu m$ for mid-IR excitation wavelength $\lambda = 2\pi c/\omega \sim 10\mu m$. Enhanced nonlinear couplings.



a) Pattern of charge displacements on the surface of a metal (upper picture) and on the surface of a 2D material (bottom picture). b) Comparison of plasmon dispersions in different systems. Dispersion in a 2D system shows a gentler dependence on wavenumber as compared to that for the interface of a 3D metal and a dielectric. (Yoon et al. Plasmonics with two-dimensional conductors. Phil. trans. Ser. A, 2014).

Retardation effects: hybridization of the plasma and light modes, $q \sim \frac{\omega}{c}$.

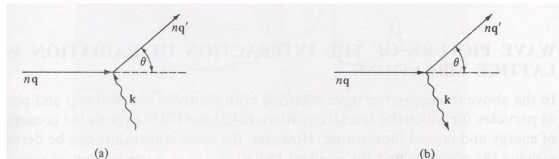
Brillouin scattering: quantum picture

Basic Idea

- Light scatters off a solid emitting or absorbing a phonon.
- Follows conservation of energy and momentum.

$$\hbar\omega' = \hbar\omega \pm \hbar\omega_s(\mathbf{k})$$

$$\hbar n\mathbf{q}' = \hbar n\mathbf{q} \pm \hbar\mathbf{k} + \hbar\mathbf{K}$$

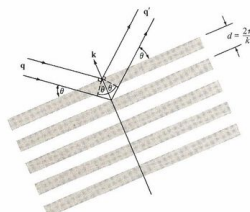


Ashcroft and Mermin

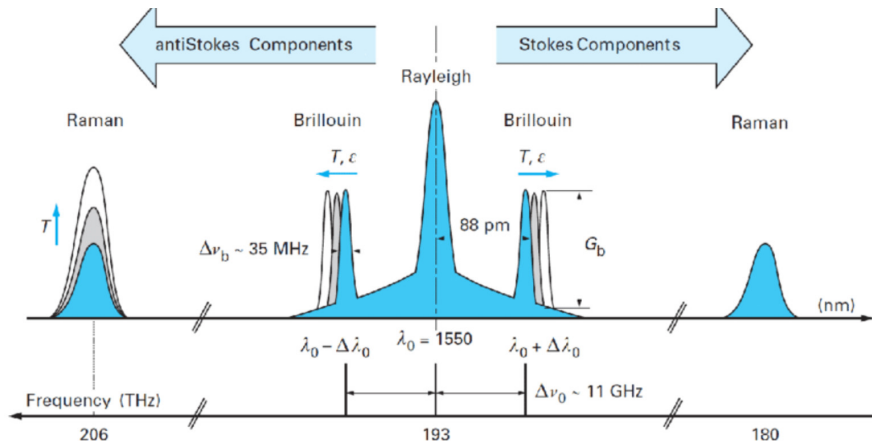
Brillouin scattering: classical picture

Classical Look at Brillouin Scattering

- Long wavelength limit allows lattice to be treated as a continuum.
- Scattering is off moving lattice distortions (phonons).
- Follows Braggs Law in the phonon's reference frame.

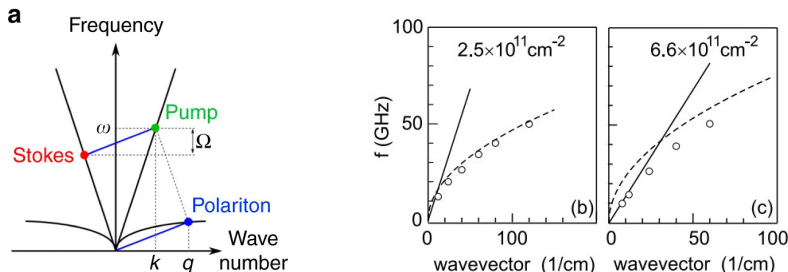


Different types of light scattering: Rayleigh, Brillouin-Mandelstam and Raman



Rayleigh, Raman and Brillouin scattering intensity in silica fibers (excitation at $1.55 \mu\text{m}$)

Collective plasma excitations in 2D electron gases probed by light scattering



The 2D-plasmon-polariton dispersion deduced from measurements for

two samples with different density. Symbols are experimental points.

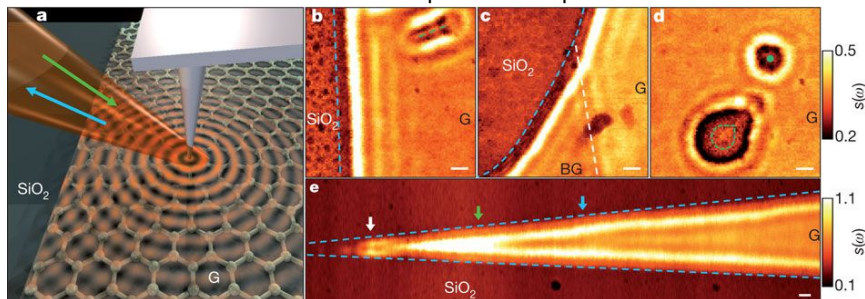
Curves are the dispersion of light (solid) and the 2D plasmon dispersion

calculated in the quasistatic approximation $\omega_p^2(q) = \frac{2\pi e^2 n_s}{m^* \epsilon(q)} q$. (Kukushkin

et al PRL 2003)

Plasmonics (photonics at the nanoscale)

Excitation and detection. Near-field optics techniques.

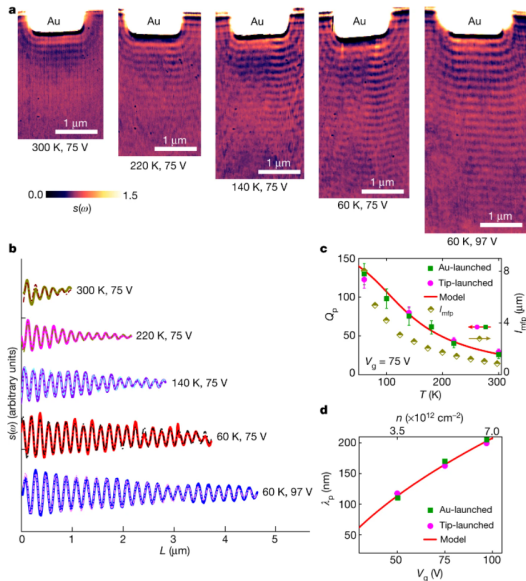


Left panel: Schematics of nano-imaging experiments. Tip launched plasmon waves interfere with themselves. Middle and Right panel: $s(\omega)$ images of graphene revealing plasmon fringe patterns close to the graphene edge (blue dashed lines), line defect (green dashed line), and boundary between graphene and bilayer graphene (Grey dashed line). In all panels, G stands for graphene, BG stands for bilayer graphene, scale bar is 100 nm. (Basov group)

Strong field confinement. Enhanced nonlinear couplings.

Plasmonics (photonics at the nanoscale)

Graphene plasmon propagation lengths $> 10\mu\text{m}$:



The Anderson-Higgs phenomenon

Collective phase oscillations in superconductors?

We'll deal with the charge-neutral superfluids first.

The dynamics of the condensate phase at long wavelengths can be captured by a simple [hydrodynamic approach](#). We combine the continuity equation for supercurrent

$$\partial_t n + \nabla \cdot j = 0, \quad j = \frac{\hbar}{m} n_s \nabla \theta$$

with the mean-field and Josephson relations, $\delta n = \delta \mu / g$, $\delta \mu = \hbar \frac{\partial \theta}{\partial t}$. This gives a wave equation:

$$\partial_t^2 \theta - \frac{gn_s}{m} \nabla^2 \theta = 0, \quad (6)$$

describing Bogoliubov sound modes with acoustic dispersion

$$\omega = sq, \quad s = \sqrt{\frac{gn_s}{m}} \quad (7)$$

Collective phase oscillations in superconductors?

The phase dynamics in charged superfluids takes on a very different form due to the Anderson-Higgs phenomenon. Namely, the phase mode becomes gapped, in a direct contradiction to the Goldstone theorem.

Indeed, superconductors got a broken gauge symmetry, and have a stiffness that leads to superconducting currents. What is the low-energy excitation? It does not have one. But what about Goldstone's theorem?

Goldstone of course had conditions on his theorem which excluded superconductors. It is just that everybody forgot the extra conditions, and just remembered that you always got a low-frequency mode when you broke a continuous symmetry. The condensed-matter physicists already knew before high-energy theorist rediscovered it for themselves why there is no Goldstone mode for superconductors; P. W. Anderson had shown that it was related to the long-range Coulomb interaction, and its absence is related to the Meissner effect.

The Anderson-Higgs phenomenon, a toy model

As a simple toy model we consider the condensate phase mode coupled to electromagnetic fields by a minimal coupling dictated by the gauge symmetry. The action is the difference of the kinetic and potential energy terms, $S = \int dt L(\theta, A, \phi) = \int dt [E_{\text{kin}} - E_{\text{pot}}]$, and L is harmonic:

$$L(\theta, A, \phi) = \int d^3x \left[\frac{\hbar^2 n_s}{2ms^2} \left(\partial_t \theta + \frac{2e}{\hbar} \phi \right)^2 - \frac{\hbar^2 n_s}{2m} \left(\nabla \theta - \frac{2e}{\hbar c} A \right)^2 + \frac{E^2}{8\pi} - \frac{H^2}{8\pi} \right]$$

with the phase mode velocity s given in Eq.(7). The EM fields are the usual functions of the EM potentials $E = -\frac{1}{c} \partial_t A - \nabla \phi$, $H = \nabla \times A$. For a charge-neutral superfluid, $e = 0$, the dynamics of the phase and of the electromagnetic potentials are decoupled. In this case, the variational principle generates the wave equation for the phase mode, Eq.(6), and Maxwell equations. This gives the acoustic phase mode dispersing as $\omega_1 = sq$, Eq.(7), and two photon modes $\omega_{2,3} = cq$, respectively.

The behavior for $e \neq 0$ can be analyzed by using the [gauge symmetry](#) to absorb θ into A and ϕ . After fixing the gauge by a gauge transformation $A \rightarrow A + c \nabla \chi$, $\phi \rightarrow \phi - \partial_t \chi$ with $\chi = \frac{\hbar}{2e} \theta$, the Lagrangian depends only on A and ϕ : $L = \int d^3x \left[\frac{4e^2 n_s}{2m} \left(\frac{1}{s^2} \phi^2 - \frac{1}{c^2} A^2 \right) + \frac{E^2}{8\pi} - \frac{H^2}{8\pi} \right]$. Analysis shows that all three modes described by this Lagrangian are [gapped](#) (see HW4).

- 1) Condensate phase and photon modes in low-dimensional superconductors ($D < 3$). Similar to plasmon oscillations, the phase mode and the two photon modes become gapless, with the $\omega \sim \sqrt{q}$ dispersion at long wavelengths.
- 2) Condensate amplitude modes $\delta|\Delta|(x, t)$
- 3) Polaritons: plasmons hybridized with photons
- 4) Magnetoplasmons: collective charge oscillations in the presence of magnetic field
- 5) Kohn's theorem: no renormalization of plasma frequency due to e-e interactions (for parabolic bands, quasi-Galilean symmetry)
- 6) Quanta of collective excitations: $\Delta E = \hbar\omega(q)$. Can this happen to a classical wave?

Next topic: the rigidity of the Fermi sea

- * Friedel oscillations
- * Kohn anomaly
- * Peierls instability (charge and spin density waves)
- * The Kohn-Luttinger superconducting pairing

The static finite-q response of a free Fermi gas

Next, consider $\omega = 0$, but keep q finite (it'll be a little cumbersome but superinteresting)

$$\Pi(q)_{\omega=0} = 2 \int \frac{d^3 k}{(2\pi)^3} \frac{f_k - f_{k+q}}{\epsilon_k - \epsilon_{k+q}} = \dots = 4 \int \frac{d^3 k}{(2\pi)^3} \frac{f_k}{\epsilon_k - \epsilon_{k+q}}$$

Let's transform it to polar coordinates $d^3 k = k^2 dk \sin \theta d\theta d\phi$,
 $\epsilon_{k+q} - \epsilon_k = \frac{kq}{m} \cos \theta + \frac{q^2}{2m}$, and integrate over $u = \cos \theta$:

$$\Pi(q) = -4 \frac{2m}{(2\pi)^2} \int_0^{k_F} dk \int_{-1}^1 du \frac{k^2}{2kqu + q^2} = -\frac{8m}{(2\pi)^2} \int_0^{k_F} dk \frac{k}{q} \ln \left| \frac{q + 2k}{q - 2k} \right|$$

Integration over $0 < k < k_F$ can be performed using the following indefinite integral:

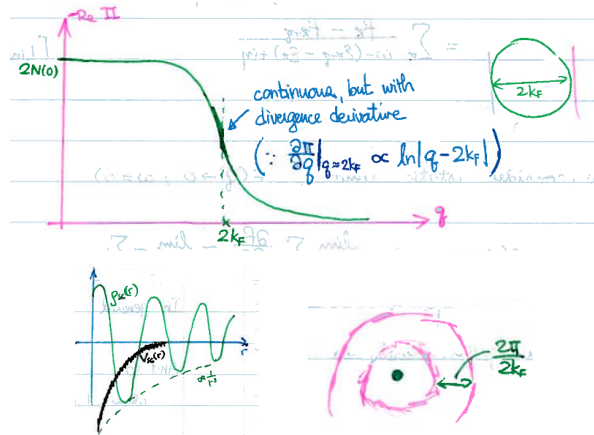
$$\int x \ln \frac{a+x}{a-x} dx = ax + \frac{1}{2}(x^2 - a^2) \ln \frac{a+x}{a-x}$$

This gives a continuous function with a derivative which is **log-divergent** at $q = 2k_F$, a manifestation of the Fermi surface “rigidity”

$$\Pi(q) = -\frac{mk_F}{2\pi^2} \left[1 - \frac{k_F}{q} \left(1 - \frac{q^2}{(2k_F)^2} \right) \ln \left| \frac{q + 2k_F}{q - 2k_F} \right| \right]$$

Rigidity of the Fermi surface: singularity at $q = 2k_F$

The qualitative picture: Fermi sea is compressible at $q \lesssim 2k_F$ and incompressible at $q \gtrsim 2k_F$. Nonanalytic polarization function $\Pi(q)$ singular at $q = 2k_F$, non-exponential oscillatory screening charge (Friedel oscillations, $1/r^3$ power law)

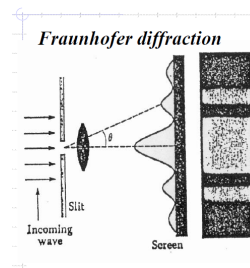


The relation between oscillations in real space and a singular behavior in k space

This can be illustrated by a familiar-to-all example from optics: the Fraunhofer diffraction of waves passing through a slit. Sharp edges of the slit create an oscillatory dependence of the diffracted wave amplitude on the scattering angle with a power-law envelop, parameterized by the wavevector component parallel to the slit plane:

$$A(k) = \int_{-a}^a d\xi e^{ik\xi} = 2 \frac{\sin ka}{k}$$

It may therefore be tempting to identify the Fraunhofer oscillations and Friedel oscillations by replacing the box function $-a < \xi < a$ by a Fermi distribution with a sharp edge at $k = k_F$ (and renaming ξ and k as electron momenta and positions). Note, however, that this simple argument misses a factor of two in the oscillation period, predicting periodicity $2\pi/k_F$ instead of π/k_F . This difference can be understood by noting that Friedel oscillations arise from pairs of particles and holes: an electron with momentum $k \sim k_F$ and a hole with momentum $k \sim -k_F$, forming particle-hole pairs with momenta q in the box $-2k_F < q < 2k_F$.



Consequences of the singularity at $2k_F$:

- (i) Friedel oscillations $\delta\rho(x) \sim \frac{\cos(2k_F|x|)}{|x|^3}$
- (ii) Surface states of metals: $2k_F$ interference imaged by scanning tunneling probes
- (iii) Softening of phonon dispersion near $q \approx 2k_F$ (Kohn anomaly)
- (iv) Stronger $2k_F$ singularity at $D = 2$ and an even stronger singularity at $D = 1 \dots \rightarrow \dots$ Peierls instabilities towards charge density wave or spin density wave. A unique example of symmetry breaking.
- (v) At $D > 1$ the system can mimic the $1D$ behavior through perfect "nesting" of the Fermi surface
- (vi) RKKY interaction: an oscillatory long-range interaction between localized spins in metals

Imaging surface states by scanning tunneling probes: quantum confinement and $2k_F$ interference

Crommie, Lutz & Eigler, Science 1993

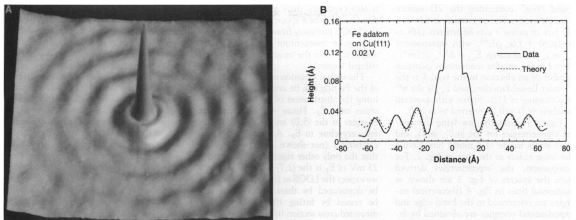


Fig. 1. (A) Constant current $130 \text{ \AA} \times 130 \text{ \AA}$ image of an Fe adatom on the Cu(111) surface ($V = 0.02$ volt, $I = 1.0$ nA). The apparent height of the adatom is $\sim 0.9 \text{ \AA}$. The concentric rings surrounding the Fe adatom are standing waves due to the scattering of surface state electrons with

the surface. (B) Solid line: average of three cross sections taken through the center of the Fe adatom image in (A). Dashed line: fit of Eq. 1 to the cross section (the data was fit only up to 18 \AA from the center of the adatom).

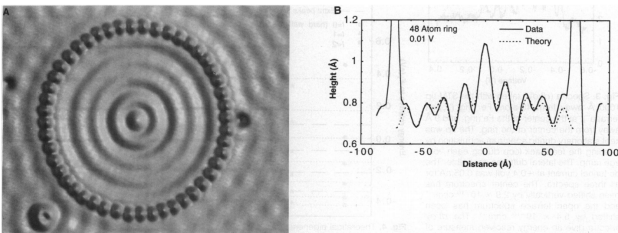


Fig. 2. Spatial image of the eigenstates of a quantum corral. (A) 48-atom Fe ring constructed on the Cu(111) surface ($V = 0.01$ volt, $I = 1.0$ nA). Average diameter of ring (atom center to atom center) is 142.6 \AA . The ring encloses a defect-free region of the surface. (B) Solid line: cross section of the above data. Dashed line: fit to cross section using a linear combination of $[5,0]$, $[4,2]$, and $[2,7]$ eigenstate densities.

Fourier transform scanning tunneling spectroscopy on the surface state of Ag(111)

Grothe et al, PRL 111, 246804 (2013)

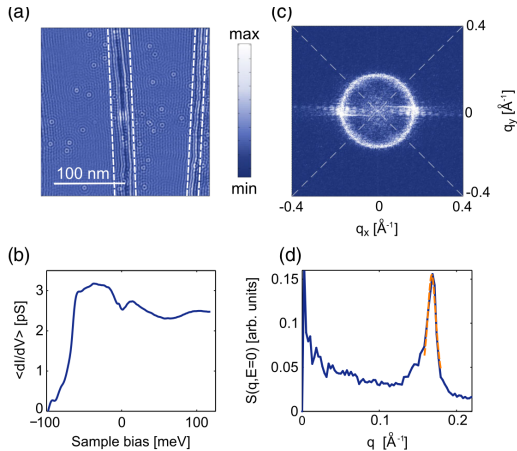


FIG. 1 (color online). (a) Conductance map (dI/dV) of a $239 \times 239 \text{ nm}^2$ area at $E = eV = 0$ meV (tip height set at $V = -100$ meV, $I = 200$ pA). LDOS modulation due to scattering at step edges and CO adsorbates are visible. The areas around the step edges indicated by white dashed lines were removed as discussed in the main text. The scale ranges from 2.3 to 3.3 pS. (b) Average dI/dV spectrum from a defect free area with a total size of 100 nm^2 . The particle-hole symmetric steps at E_F likely originate from an inelastic co-tunneling pathway via phonon modes polarized perpendicular to the surface. (c) Absolute value of the Fourier transform (power spectrum) of the dI/dV map ($E = 0$, panel a) showing a ring with radius $q = 2k_F$, where \mathbf{q} is the scattering vector. The increased intensity along the q_x direction originates from the step edge contributions. (d) The QPI line profile $S(|\mathbf{q}|, E = 0)$. The scattering peak is slightly asymmetric with an enhanced intensity at low \mathbf{q} , which is more pronounced at higher energies.

FTSTS technique to obtain constant energy maps and band dispersion using a local measurement: [Simon et al 2011](#)

Berry phase and wave interference: [Dutriex et al. 2019](#)

Kohn anomaly and Peierls instability

Kohn anomaly: $2k_F$ -softening of phonon dispersion

Longitudinal acoustic phonons coupled to electrons (a toy model).

Dynamics of an elastic continuum? Displacement field harmonics

$u(x, t) = \sum_q e^{iqx} u_q(t)$; The canonical action $A = \int dt(K - P)$:

$$A = \int dt \int d^3x \frac{\rho}{2} (\partial_t u)^2 - \frac{K}{2} (\nabla \cdot u)^2 = \sum_q \int dt \frac{\rho}{2} \partial_t u_{-q} \partial_t u_q - \frac{Kq^2}{2} u_{-q} u_q$$

From $\delta A / \delta u = 0$ obtain the wave equation $\rho \partial_t^2 u - K \nabla^2 u = 0$ and the

"bare" acoustic phonon dispersion relation $\omega = sq$, $s = \sqrt{K/\rho}$.

Add the coupling between phonons and electrons through deformation potential $H_{el-ph} = \int d^3x g \nabla u \delta n(x)$. This alters the wave equation as

$$\rho \partial_t^2 u - K \nabla^2 u - g \nabla \delta n(x) = 0$$

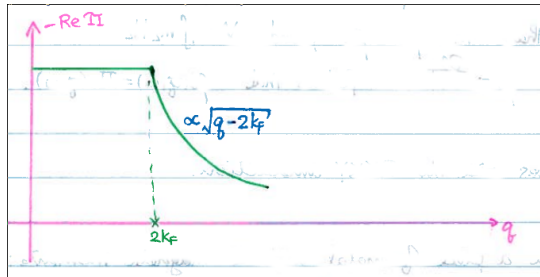
To close the loop, we note that the response of electrons to the deformation potential $U = g \nabla \cdot u$ is given by the free-fermion polarization function. For Fourier harmonics, $\delta n_{q,\omega} = \Pi(q, \omega) U_{q,\omega}$. Actually, since phonons are slow, $s \ll v_F$, we can use static response $\Pi(q)_{\omega=0}$. This gives a dispersion relation which is **softened by the coupling to electron polarization**:

$$\omega^2 = q^2(s^2 + \lambda \Pi(q)), \quad \lambda = g^2 / \rho$$

The softening is strongest near $q \approx 2k_F$, and depends on the q direction

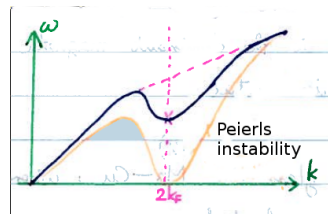
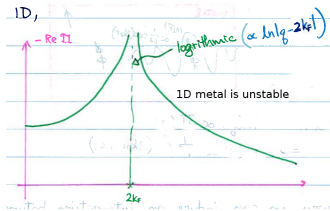
for anisotropic FS. KA's are **ubiquitous**, used to map out Fermi surfaces!

Singularity at $q = 2k_F$ in dimensionality 2 and 1



In 2D the manifestations are stronger than in 3D yet similar overall.

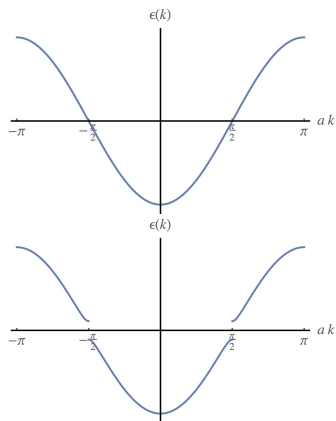
Much more interesting in 1D: softening at $2k_F$ diverges as a $\log |q - 2k_F|$, leads to instability: period-doubling or incommensurate density waves



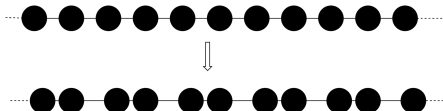
Peierls instability of a 1D metal

Peierls' theorem: a one-dimensional equally spaced chain with one electron per ion is unstable.

Gap opening at half BZ boundary:

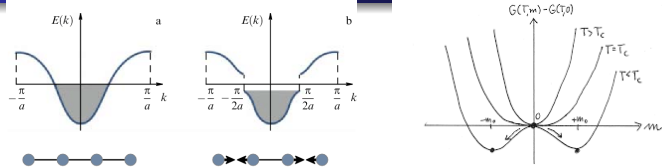


Distortion of atoms with period doubling creates a modulation that Bragg-scatters between the Fermi points $+k_F$ and $-k_F$ (right-movers and left-movers)



Peierls instability occurs in 1D and quasi-1D metals such as polyacetylene $[C_2H_2]_n$, organic semiconductors (TTF TCNQ), many other systems

Peierls instability: analogy with the BCS theory



In Peierls' transition to a state with a gap Δ opening at $\pm k_F$ the electron subsystem gains a logarithmically-large energy

$$\delta E_{\text{el}} = \sum_k f(k) (\epsilon_0(k) - (\epsilon_0^2(k) + \Delta^2)^{1/2}) \sim -\frac{1}{2} N(0) \Delta^2 \log \frac{W}{|\Delta|}.$$

At the same time, the phonon subsystem loses energy $\delta E_{\text{ph}} \sim \frac{1}{2g} \Delta^2$.

Comparing δE_{el} and δE_{ph} we conclude that the insulating gapped state is always lower in energy than the metallic gapless state. The total energy $W = \delta E_{\text{el}} + \delta E_{\text{ph}}$ dependence on Δ is of a classic double-well form invariant under sign reversal $\Delta \rightarrow -\Delta$. Spontaneous symmetry breaking: distinct, but equivalent, even and odd dimerized states. The gap found from minimizing W in Δ is of a BCS form:

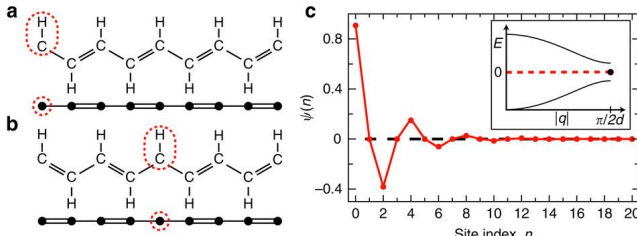
$$\Delta \sim W e^{-1/gN(0)},$$

Therefore, no threshold for the instability. Namely, a 1D metal is always unstable at low enough temperatures.

Peierls instability in 1D and quasi-1D electron bands

a) quasi-1D systems: There are many materials that are built of weakly coupled molecular chains, where electrons can move freely along the direction of the chains, but motion is restricted perpendicular to the chains. These systems can exhibit a large variety of strongly-correlated phases: charge-density waves, spin-density waves, 1D superconductivity. Electron densities at which CDW, SDW and SC states occur can be commensurate or incommensurate with the crystal lattice. NbSe_3 and $\text{K}_{0.3}\text{MoO}_3$ are two examples in which charge density waves have been observed at relatively high temperatures of 145 K and 180 K, respectively. Here is a good review: [Charge-density-wave conductors, by Rob Thorne](#)

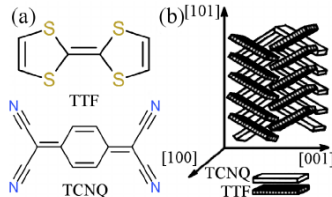
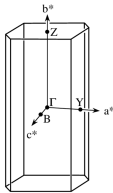
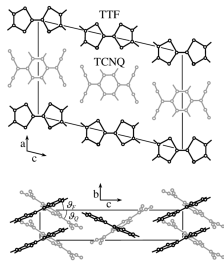
b) The dimerized state in polyacetylene $[\text{C}_2\text{H}_2]_n$; SSH model; topological bands, zero-energy states at domain boundaries; fractional-charge solitons. Relation to Peierls' instability: [term paper](#) and [presentation slides](#) (Alex Strelnikov '12). See also 8.511 class notes



Quasi-1D conductors (TTF TCNQ, Tetrathiofulvalene Tetracyanoquinodimethane)

A large variety of strongly correlated Peierls-like phases: CDW, SDW, SC, exotic Quantum Hall states.

Luttinger liquid phases: the 1D nature of the material causes a breakdown of the Fermi liquid theory for electron behavior. A Luttinger liquid is a paramagnetic one-dimensional metal without Landau quasi-particle excitations.



Peierls instability summary

- Two main types of density wave order, commensurate and incommensurate. Schematically,

$$\rho(x) = u_0 \cos(2\pi x/a) + \delta u \cos(qx + \theta), \quad q = 2k_F$$

Can be charge density, spin density, superfluid pair density, etc.

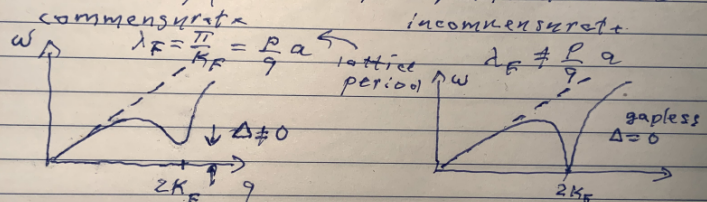
- Commensurate order: $qa = 2\pi \frac{1}{2}, 2\pi \frac{m}{n}$. Phase θ is locked, several discrete values. Discrete symmetry breaking, topologically ordered domains (Berry phase as in SSH model), zero modes at the domain boundaries, fractionalized charge.
- Incommensurate order: $qa/2\pi$ an irrational number. Phase θ is free (not locked), a continuous symmetry breaking. A new dynamical variable, somewhat similar to the order parameter phase in superfluids. New collective excitations – phasons – with interesting dynamics (a rich playground for nonlinear transport).
- Peierls instability is an example of dynamically generated topological order (a band with Berry phase winding and other attributes). Mathematically isomorphic to BCS theory.

Phonons in the Peierls-ordered state

Peierls order types

Commensurate & Incommensurate

charge and spin density wave states
mediated by phonons and/or spin fluctuations



	comm	incomm
phonons	gapless	$\Delta = 0$
phasons (2K_F phonons)	$\Delta \neq 0$	$\Delta = 0$
solitons, midgap states	$\Delta' \neq 0$	-
	semicond.	correlated metal
	$R(T \rightarrow 0) \rightarrow \infty$	

The Kohn-Luttinger superconductivity mechanism

- Can superconductivity arise due to repulsive interactions? Can electron-electron interactions lead to pairing?
- It has been known from the early 1950s that screened Coulomb potential has a long-range oscillatory tail $\cos(2k_F r + \phi_0)/r^3$ at large distances $r k_F \gg 1$ (often called Friedel oscillations).
- Due to these oscillations, the screened Coulomb interaction gets over-screened at some distances and becomes attractive.
- Analyze the pairing at non-zero orbital momentum l of Cooper pairs: the pairing problem decouples between different l :

$$V(\mathbf{k} - \mathbf{k}') = \sum_{l,m} V_{l,m} Y_{l,m}^*(\mathbf{k}') Y_{l,m}(\mathbf{k}), \quad |\mathbf{k}'|, |\mathbf{k}| = k_F$$

(using the addition theorem for spherical harmonics).

- Because of this decoupling, even if only one partial component of the interaction is attractive, $V_{l,m} < 0$, and all other are repulsive, the system still undergoes a pairing instability into a state with l for which the interaction is attractive.

The Kohn-Luttinger superconductivity mechanism

- Kohn and Luttinger (1965) considered the fully screened interaction $V(k) = V_0(k)/\epsilon(k)$, $\epsilon(k) = 1 - V_0(k)\Pi(k)$ and linked the interactions $V_{l,m}$ to the nonanalytic parts of $\Pi(k \approx 2k_F)$ ($V_{l,m} \sim 1/l^4$ and sign-changing).
- KL applied their results to superfluidity ${}^3\text{He}$ (not yet discovered at the time). Focusing on pairing with $l = 2$ they predicted a very low critical temperature $T_c \sim 10^{-17}$ K.
- In 1968, Fay and Layzer extended KL calculations to $l = 1$, which a few years later (in 1972) was found experimentally to be the actual pairing state in ${}^3\text{He}$. For p-wave, the KL result for T_c is $\sim 10^{-3}$ K, which by order of magnitude is the same as experimental $T_c \sim 2.5 \times 10^{-3}$ K (though the actual pairing glue is believed to be due to spin fluctuations).
- The $2k_F$ nonanalytic part of interaction is stronger in lower space dimension, making the KL effect quite strong in $D = 2$ and $D = 1$.
- Viable mechanism for superconductivity with unconventional (non s-wave) pairing and high T_c . Many examples: cuprate SC (d-wave pairing), pnictides (s_{\pm} pairing, multicomponent Fermi surfaces), heavy-fermion systems, twisted bilayer graphene (?)

The KL pairing mechanism: questions

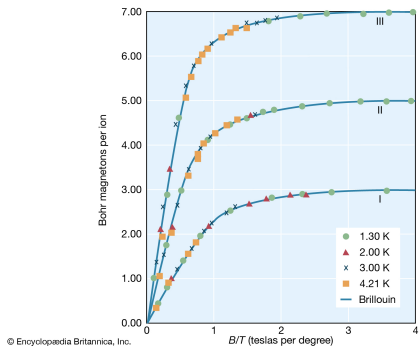
- Q: Coulomb interaction is pair-breaking in the s-wave pairing channeling. Why then in most SC metals pairing is s-wave?
- A: Indeed, Coulomb repulsion is typically stronger than phonon attraction. However, phonon attraction involves considerable retardation whereas Coulomb interaction is practically non-retarded (on \hbar/E_F time scales). As a result, phonon attraction wins. Namely, $\lambda = \lambda_{ph} - \lambda_{ee}/\log(E_F/\omega_D) > 0$
- Q: What are the observable signatures of topological superconductivity (phase of Δ winding around the Fermi surface)
- A: 1) chiral edges modes capable of heat conduction. Compare to s-wave superconductors that do not conduct heat. 2) Zero-energy Majorana modes at vortex cores, gapless chiral Majorana modes propagating at system edge and phase boundaries.

Magnetism

Need for Quantum Exchange; Why magnetism is quantum

- The word “quantum” in the title is almost redundant, as a simple argument — the Bohr – van Leuwen theorem — demonstrates.
- Indeed, the classical partition function of charged particles coupled to a B field through magnetic vector potential is B -independent!
- $Z_{B \neq 0} = \int d^3p d^3r e^{-\beta H(p - eA(r))}$. But this equals $Z_{B=0}$ after redefining $p' = p - eA(r)$ (since p and r commute in classical theory)
- No magnetism in classical theory
- Something quantum mechanical is required
- Yet, magnetostatic interactions are too weak. They are present in magnetic materials but mostly irrelevant (except for relatively weak anisotropy effects)

A reminder: magnetism in gases



© Encyclopaedia Britannica, Inc.

Magnetization of paramagnetic substances: The approach to saturation in the magnetization of a paramagnetic substance following a Brillouin curve. Curves I, II, and III refer to different ions for which $g = 2$ and $j = 3/2, 5/2$, and $7/2$, respectively.

Quantum Exchange

- The interactions which provide such strong interactions between magnetic moments are nothing to do with the magnetic nature of the spin degree of freedom, but are to do with its symmetry properties.
- They exist because of the connection between symmetry of spin and spatial wavefunctions for electrons as fermions, and so the energy scales associated with these interactions are the energy scales of the spatial degrees of freedom
- The key players are the electronic kinetic energy and Coulomb interaction.
- To summarize briefly; a given spin configuration restricts the range of possible spatial configurations, and because different spatial configurations can have significantly different energies, there is thus a large energy associated with different spin configurations.

Quantum Exchange

- Within this general framework, there exist two categories of types of magnetic interaction:
- Direct (potential) exchange This is driven by minimizing potential energy, by reducing wavefunction overlap. The overlap is reduced by adding nodes to the wavefunction, producing antisymmetric spatial wavefunctions, and so favors symmetric spins, i.e. **ferromagnetic interactions**. This case arises when electrons occupy wavefunctions that overlap in space.
- Kinetic exchange. This is driven by minimizing kinetic energy, by reducing gradients of wavefunctions, i.e. allowing delocalization of electrons. This corresponds to using symmetric superpositions of wavefunctions, and so favors antisymmetric spins, i.e. **antiferromagnetic interactions**. This case generally arises for localized electronic orbitals

Ferromagnetic order: The mean field approach

- Heisenberg model for spin variables on a lattice

$$H = -\frac{1}{2} \sum_{x \neq x'} J(x - x') \hat{s}_x \hat{s}_{x'}, \quad J(x - x') > 0$$

Ground state at $T = 0$: all spins aligned. Describe the phase transition?

- The Curie-Weiss ("molecular field") method. Start with a single spin in an external field $H = -h\hat{s}_z$. Ensemble-averaged magnetization is found as $m = \langle \hat{s}_z \rangle = L_J(\beta h) = \dots = \left(\sum_{m=-j}^{m=j} m e^{\beta hm} \right) / \left(\sum_{m=-j}^{m=j} e^{\beta hm} \right)$.
- For spin-1/2 case, $j = 1/2$ and $m = \tanh \beta h / 2$.
- For many spins, consider one spin (s_x) in an effective field of all other spins, $h_x = \sum_{x'} J(x - x') s_{x'}$. Replacing spins by their average values, have

$$h = Um, \quad m = L_J(\beta h)$$

where $U = \sum_{x'} J(x - x')$. Ensemble average in partition function.

- The equation $m = L_J(\beta Um)$ has zero solution at $\beta U < 1$ and nonzero solutions at $\beta U > 1$. The critical temperature $T_c = U$.
- Susceptibility $\chi = \frac{\partial m}{\partial h} \sim \frac{1}{T - T_c}$ (Curie-Weiss law). Divergence at T_c .

Antiferromagnetic order: The mean field approach

- Heisenberg model for spin variables on a lattice

$$H = -\frac{1}{2} \sum_{x \neq x'} J(x - x') \hat{s}_x \hat{s}_{x'}, \quad J(x - x') < 0$$

Ground state: two sublattices, spins aligned on each sublattice, antialigned on different sublattices. Phase transition?

- The Curie-Weiss ("molecular field") method. Start with a single spin in an external field $H = -h\hat{s}_z$. Ensemble-averaged magnetization is found as $m = \langle \hat{s}_z \rangle = L_J(\beta h) = \dots$.
- For spin-1/2 case, $j = 1/2$ and $m = \tanh \beta h / 2$.
- For many spins, consider one spin (s_x) in an effective field of all other spins, $h_x = \sum_{x'} J(x - x') s_{x'}$. Replacing spins by their average values, $+m$ on one sublattice, $-m$ on another sublattice, have

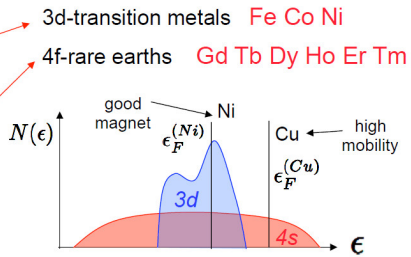
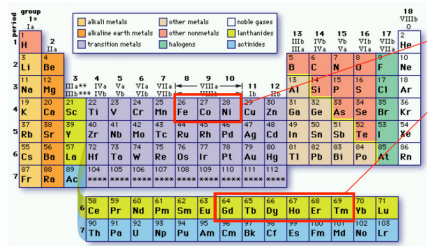
$$h = Um, \quad m = L_J(\beta h)$$

where $U = \sum_{x'} (+/-) J(x - x')$.

- The equation $m = L_J(\beta Um)$ has zero solution at $\beta U < 1$ and nonzero solutions at $\beta U > 1$. The critical temperature $T_c = U$.
- Susceptibility $\chi = \frac{\partial m}{\partial h} \sim \frac{1}{T + T_c}$ (Néel law). No divergence at T_c .
- Validity: small fluctuations, large spin j

Intinerant magnetism: Stoner instability of band electrons

- A magnetic phase transition of a Fermi liquid with net non zero magnetization
- There can be other magnetically ordered states with no net magnetization (eg. AFM) . General class of magnetic transitions is specified by ordering wave vectors \vec{Q} . Also includes Spin Density Waves
- Will focus here on Ferromagnetic Instability. A simple illustration of QPT
- Phase transition occurs on varying a system parameter (Coulombic repulsion U in Stoner case)

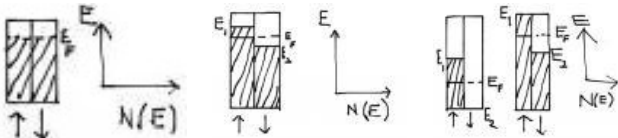


What is Stoner instability?

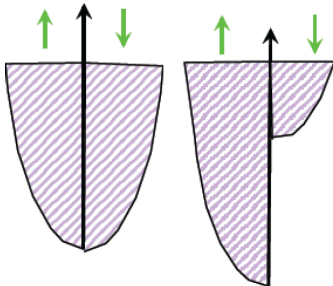
- Consider a 3d transition metal, in which the 3d electrons give rise to magnetism; since the electrons are itinerant (and delocalized) in the metal, the magnetism stems from 3d electron bands.
- The band itself consists of two sub-bands — one for up-spin electrons and another for down-spin electrons. If there are less than ten 3d-electrons in the system, the 3d-band will be partially filled. Further, if the system fills these bands without discrimination, then both the sub-bands will be equally filled.
- If suppose we can define an interaction energy which indicates a reduction in energy if the electrons from one of the sub-bands, say those corresponding to down-spin can be transferred to the up-spin band, then, under certain circumstances it can be shown that this will lead to an instability as discussed below.
- What prevents such an emptying of one of the sub-bands in favor of another is the resultant increase in the electron kinetic energy
- In fact, the total variation in energy in such sub-band transfer of electrons can be shown to be equal to $\Delta E = \frac{n^2 p^2}{N(E_F)} [1 - U_{\text{eff}} N(E_F)]$, where, n is the total number of 3d electrons per atom, p is the fraction of atoms that move from down-spin sub-band to up-spin sub-band, U_{eff} is the effective interaction energy, and $N(E_F)$ is the density of energy states at the Fermi level.

What is Stoner instability?

- Thus, if the quantity in square brackets is positive, the state of lowest energy corresponds to $p = 0$ — or, in other words, the metal is non-magnetic. However, if the quantities in the square bracket is negative, the band is “exchange split” — $p > 0$, and hence the metal is ferromagnetic.
- This is known as the Stoner instability, or sometimes ferromagnetic instability. From the equation, it is clear that such band splitting is favored for large exchange interaction energy as well as for large density of states. Since the density of states for s- and p-bands are considerably smaller, which, in turn explains why such band magnetism is restricted to elements with partially filled d-band.
- Here are the schematics explaining band magnetism in partially filled d-electron systems: paramagnetic, weak ferromagnetism, strong ferromagnetism ($n < 5$ and $n > 5$)

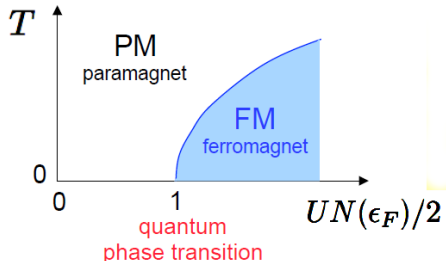


Hubbard model



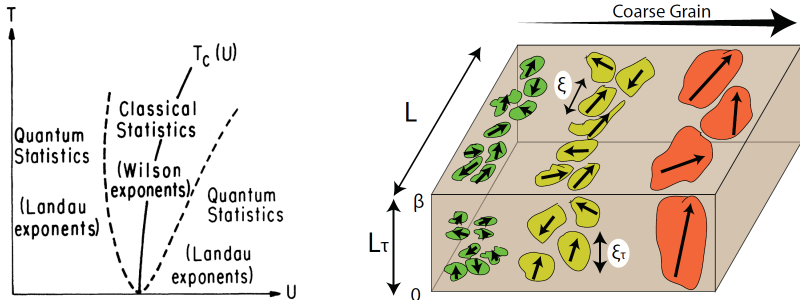
- Hubbard model $\mathcal{H}_{hubbard} = -t \sum_{\langle ij \rangle} c_i^\dagger c_j + U \sum_i n_{i\uparrow} n_{i\downarrow}$
- Electrons reduce U by favoring magnetic ordering
- Cost: Gain in Kinetic energy

Phase diagram and instability criterion



- Instability occurs when $UN(\epsilon_F)/2 > 1$ (The mean-field approximation).
- Ferromagnetic order at $U > U_c$
- Near critical point spin response function $\chi(q, \omega)$ diverges for $q, \omega \rightarrow 0$
- The selfconsistent approach to evaluate $\chi(q, \omega)$

Extend from $T = 0$ to finite T : a quantum critical point



- Fluctuations and scaling at the QCP
- Quantum vs. Classical: Classical $d \leftrightarrow d + 1$
- Close analogy with a ‘finite’ classical system. A box with infinite d dimensions and a finite $d + 1$ th dimension

The Hubbard model and Mott insulators

- The Hubbard model is a toy model designed to capture the essence of the magnetic effects due to Coulomb interactions. A tight-binding Hamiltonian with the long-range Coulomb interaction replaced by an on-site repulsion (on a square lattice)

$$H = -t \sum_{(ij),\sigma} (c_{i\sigma}^\dagger c_{j\sigma} + c_{j\sigma}^\dagger c_{i\sigma}) + U \sum_j n_{j\uparrow} n_{j\downarrow}, \quad n_{j\sigma} = c_{j\sigma}^\dagger c_{j\sigma}$$

- Note that the Pauli exclusion allows double occupancy only by pairs of electrons of opposite spin; repulsion U penalizes double occupancy.
- The hopping (t) term tends to delocalize electrons through hopping and competes with the interaction (U) term.
- Despite that this model is an extreme simplification, it has resisted the exact solution in dimension $d > 1$
- We'll discuss the features of the physics in the limits that are well understood: $U = 0$, $U = \infty$, large U/t ; with the density at and near half-filling, $n = n_\uparrow + n_\downarrow \approx 1$

The Hubbard model and Mott insulators

$$H = -t \sum_{(ij),\sigma} (c_{i\sigma}^\dagger c_{j\sigma} + c_{j\sigma}^\dagger c_{i\sigma}) + U \sum_j n_{j\uparrow} n_{j\downarrow}$$

- We begin our analysis with the case of half-filling ($= n_{j\uparrow} + n_{j\downarrow} = 1$)
- In the weak repulsion limit, $U = 0$, the ground state is a Slater determinant made of the free-particle plane wave states each containing two electrons of opposite spin:

$$|\Psi\rangle = \prod_{k,\sigma=\uparrow,\downarrow} \psi_{k\sigma}^\dagger |0\rangle, \quad \psi_{k\sigma}^\dagger = \frac{1}{\sqrt{N}} \sum_{j=1}^N e^{ikR_j} c_{k\sigma}^\dagger$$

- This is an ordinary nonmagnetic ground state, representing a metallic ground state
- Consider now the case $U = \infty$ for which there can be no double occupancy. Here the state must be of the form

$$|\Psi\rangle = \left(\prod_{j=1}^N c_{j\sigma_j}^\dagger \right) |0\rangle, \quad \sigma_j = \uparrow \text{ OR } \downarrow$$

There are 2^N different states according to the choice of spin orientation on each lattice site.

The Hubbard model and Mott insulators

- Since the particles cannot hop to any neighboring sites both the kinetic energy and the interaction energy vanish. The energy eigenvalue is zero and is 2^N -fold degenerate.
- Because of this degeneracy, no particular magnetic order is favored over any other and the system is effectively a nonmagnetic insulator with an infinite charge excitation gap.
- This is a new type of insulator we have encountered. Previously we encountered insulators that can be understood with a free-electron band picture. Such interaction-induced insulators are collectively known as Mott insulators
- Zero compressibility $dn/d\mu = 0$ as for a band-gap insulator but at a “nominally metallic” band filling $1/2$ of an infinite- U Hubbard model
- A parent state for cuprate high- T_c superconductors

The half-filled infinite- U Hubbard model

- Consider what happened if we remove a single electron from this half-filled band. In this case the ground state is given exactly by

$$|\Psi\rangle = \left(\prod_k \psi_{k\uparrow}^\dagger \right) |0\rangle$$

where the product runs over all allowed k s except a single one corresponding to the highest kinetic energy

- This state is therefore a fully ferromagnetic single Slater determinant with spin $S = \frac{1}{2}(N - 1)$ and degeneracy $2S + 1$
- This is an eigenstate (since the interaction term vanishes), known as the Nagaoka state
- This is also a ground state (the Nagaoka theorem). Automatically avoids double occupancy because all spins are aligned. The kinetic energy is optimized due to the presence of a hole
- Frustrated states disfavored by the hole stirring effects.

The half-filled infinite- U Hubbard model

- Back to half-filled Mott-insulating state. Consider a large but not infinite U . Now the charge gap is finite and different spin states aren't exactly degenerate.
- It turns out that the ground state has antiferromagnetic Néel order for the square and cubic lattices
- To see how this comes about let's analyze a Hubbard model with only two electrons and two sites (can generalize later)
- States in a two-site Hubbard model:

$$|\uparrow;\uparrow\rangle \quad |\downarrow;\downarrow\rangle \quad |\uparrow;\downarrow\rangle \quad |\downarrow;\uparrow\rangle \quad |\downarrow,\uparrow;-\rangle \quad |-, \downarrow\uparrow\rangle$$

- Perturbation theory carried out in a way that is backwards to the usual one, since $U/t \gg 1$. The unperturbed Hamiltonian is the potential energy $V = U \sum_j n_{j\uparrow} n_{j\downarrow}$ and the kinetic energy $T = -t \sum_{(ij),\sigma} (c_{i\sigma}^\dagger c_{j\sigma} + c_{j\sigma}^\dagger c_{i\sigma})$ will be a perturbation.
- Since V commutes with the total spin $S = S_1 + S_2$ its eigenstates can be labeled by their total spin quantum number $S = 0, 1$
- A triplet and a singlet, both with energy $\epsilon = 0$, and two singlets with energy $\epsilon = U$ because of double occupancy.
- These are all exact eigenstates of V . We are interested in the low-energy states (assuming $U \gg k_B T$)

The half-filled infinite- U Hubbard model

- Because the kinetic energy also commutes with S , $[T, S] = 0$, the perturbation can only mix singlet states among themselves
- The low energy singlet and triplet states obey $\langle \psi | T | \psi \rangle = 0$ (In fact the triplet state is an eigenstate of H)
- Level repulsion will drive the low-energy singlet downwards, lifting the spin degeneracy and leading to an effective antiferromagnetic low-energy spin Hamiltonian

$$H_{\text{eff}} = JS_1 \cdot S_2 + C$$

with $J > 0$ and C a constant.

- To calculate J and C perturbatively in $t/U \ll 1$ note that

$$T|\psi_0\rangle = -2t \frac{1}{\sqrt{2}}(|\psi_{0L}\rangle - |\psi_{0R}\rangle)$$

so the second-order energy shift for $|\psi_0\rangle$ equals

$$\Delta\epsilon = \frac{|\langle \psi_{0L} | T | \psi_0 \rangle|^2}{-U} + \frac{|\langle \psi_{0R} | T | \psi_0 \rangle|^2}{-U} = -\frac{4t^2}{U}$$

- The energy of the triplet state remains zero, but **partial delocalization** of the electrons in the singlet case reduces the kinetic energy from zero to $\epsilon = -\frac{4t^2}{U}$

The half-filled infinite- U Hubbard model

- These results allow us to determine J and C using

$$H_{\text{eff}} = JS_1 \cdot S_2 + C = \frac{1}{2} \left[(S_1 + S_2)^2 - \frac{3}{2} \hbar^2 \right] + C$$

- This yields $\epsilon_1 = \frac{J}{4} + C$ for the triplet state, and $\epsilon_0 = -\frac{3J}{4} + C$ for the singlet state. Therefore

$$C = -\frac{t^2}{U}, \quad J = \frac{4t^2}{\hbar^2 U}$$

- For the case of an infinite lattice one obtains an effective Heisenberg spin Hamiltonian

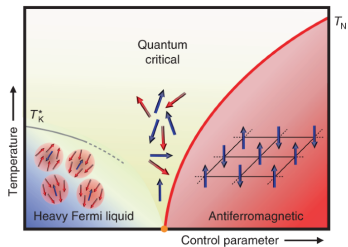
$$H_{\text{eff}} = J \sum_{(ij)} S_i \cdot S_j$$

Since the 2nd order perturbation couples only nearest neighbors this result is independent of lattice geometry and spatial dimension

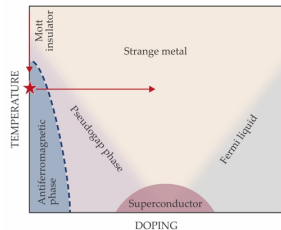
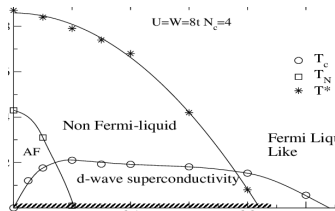
- Discuss once more the sign of the exchange interaction: Here J has its origin in the desire of the electrons to lower their kinetic energy through delocalization. This gives an **antiferromagnetic coupling**.
- In the case of Stoner instability, the Coulomb energy is lowered due to the so-called direct exchange, and the kinetic energy goes up. In this case the coupling is of a **ferromagnetic sign**.

Discuss doped Mott antiferromagnets

Nagaoka theorem: holes polarize AFM state, become magnetic polarons; at a finite doping a Fermi liquid Phase diagram:



Possible relation to the phase diagram of high- T_c superconductors.
Phase diagrams:



Magnetically ordered states and spin-wave excitations

- Consider a fully polarized ferromagnetic state

$$|S, S\rangle = |\uparrow\uparrow\uparrow\uparrow\uparrow \dots \uparrow\rangle$$

with $S = N/2$, $S_z = N/2$.

- To see that it is an eigenstate let's rewrite the Hamiltonian as

$$H = J \sum_{(ij)} \mathbf{S}_i \cdot \mathbf{S}_j = J \sum_{(ij)} \left[S_i^z S_j^z + \frac{1}{2} (S_i^- S_j^+ + S_i^+ S_j^-) \right], \quad J < 0$$

- Generate more states by applying $S^- = \sum_j S_j^-$ to $|S, S\rangle$:

$$S^- |S, S\rangle = |S, S-1\rangle = |\downarrow\uparrow\uparrow\uparrow\dots\uparrow\rangle + |\uparrow\downarrow\uparrow\uparrow\dots\uparrow\rangle + \dots + |\uparrow\uparrow\uparrow\uparrow\dots\downarrow\rangle$$

This state is degenerate with $|S, S\rangle$ because $[H, S^-] = 0$

- A simple modification of the lowering operator can be used to generate an exact spin-wave excited state

$$S_q^- = \frac{1}{\sqrt{N}} \sum_{j=1}^N e^{-i\mathbf{q}\cdot\mathbf{R}_j} S_j^-$$

$S_q^- |S, S\rangle$ an eigenstate!

- Excitation energy $\epsilon_q = \frac{\hbar^2 z}{2} |J|(1 - \gamma_q)$ with $\gamma_q = \frac{1}{z} \sum_{\delta} e^{-i\mathbf{q}\cdot\delta}$
- Magnons (spin waves):** Collective excitations, elementary excitations, or quasiparticles. Localized spins holding hands. Transporting spin, momentum and energy.

Magnetically ordered states and spin-wave excitations

- Solid as a gas: magnons behave as (nearly) free particles with Bose statistics. Similar to phonons and photons.
- Magnons in FM are soft modes: $\epsilon_q \rightarrow 0$ when $q \rightarrow 0$
- Mode softness originates from $SU(2)$ symmetry of the Hamiltonian which is spontaneously broken in the ordered state (Nambu-Goldstone theorem)
- Thermal spin fluctuations suppressing long-range order
- At low $T > 0$ estimate magnetization of the ground state using a free boson approximation:

$$M = N/2 - \sum_j b_j^\dagger b_j = N/2 - \sum_q b_q^\dagger b_q = N/2 - \sum_q n_B(\epsilon_q)$$

- with magnon bose operators $b_q^\dagger = \frac{1}{\sqrt{N}} \sum_{j=1}^N e^{-iqR_j} b_j^\dagger$ and $b_q = \frac{1}{\sqrt{N}} \sum_{j=1}^N e^{iqR_j} b_j$ obeying bosonic algebra

$$[b_q^\dagger, b_{q'}] = \delta_{qq'}, \quad [b_q^\dagger, b_{q'}^\dagger] = [b_q, b_{q'}] = 0$$

Magnetically ordered states and spin-wave excitations

The lower critical dimension (Hohenberg-Mermin-Wagner theorem)

- At low T only long wavelength magnons are excited, $\epsilon_q = Aq^2$ with A a constant

$$M = N/2 - N \int_{BZ} \frac{d^d q}{(2\pi)^d} \frac{1}{e^{\beta\epsilon_q} - 1}$$

- At $d = 3$ a weak suppression,

$$M = N/2 - CN(T/T_c)^{1/2};$$

- At $d = 2$ a log-divergence:

$$M = N/2 - CN \log(T_c/T)$$

- The HMW theorem: no long-range order at $d \leq 2$ in systems with continuous symmetry
- Seminal exception: topological phase transition in a 2D XY magnet (governed by vortices and antivortices binding/dissociating through Berezinskii-Kosterlitz-Thouless mechanism)

Topological excitations: Magnetic skyrmions

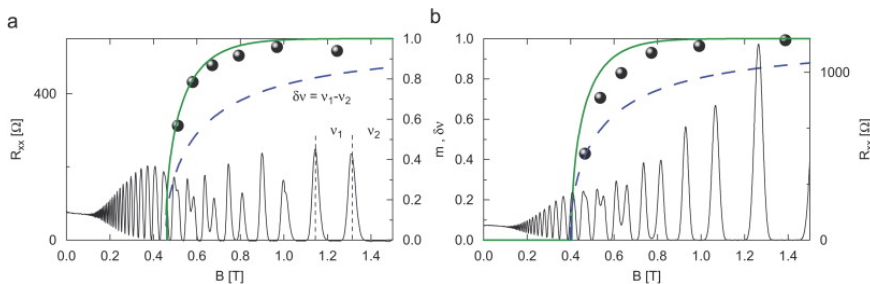


- The long-wavelength degrees of freedom of a Heisenberg ferromagnet in 2D: spin waves only?
- Magnetization slowly varying in space: $\mathbf{m}(x, y)$
- Energy from gradient expansion: $E = \int dxdy \frac{1}{2} J(\partial_\mu \mathbf{m}^\nu)^2$
- Topological invariant: the “wrapping” number (Pontryagin index)
$$n = \frac{1}{4\pi} \int \mathbf{m} \cdot \left(\frac{\partial \mathbf{m}}{\partial x} \times \frac{\partial \mathbf{m}}{\partial y} \right) dxdy$$
- Skyrmions: hedgehog-like textures stabilized by topology.
Lowest-energy skyrmions, $n = \pm 1$
- Skyrmion energy finite, $E \sim J < \infty$. Therefore, skyrmions are thermally activated at any $T < T_c$. No topological phase transition.
Finite correlation length $\xi < \infty$ and a long-range-disordered state.

This page intentionally left blank

Magnetic-field-induced Stoner transitions

- * Interaction-enhanced lifting of the electron spin degeneracy in the integer quantum Hall effect
- * A Quantum Hall Ferromagnet state in GaAlAs quantum wells



B. A. Piot, et al., Phys. Rev. B 72, 245325 (2005)

Magnetic-field-induced Stoner transitions

Spin-valley Quantum Hall Ferromagnet states in graphene monolayers at charge neutrality (four-fold splitting of the Dirac $n = 0$ Landau level)

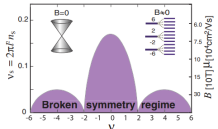
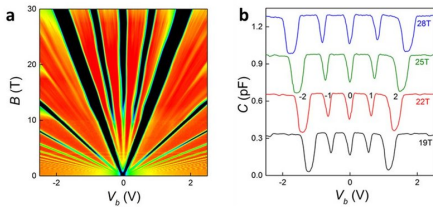
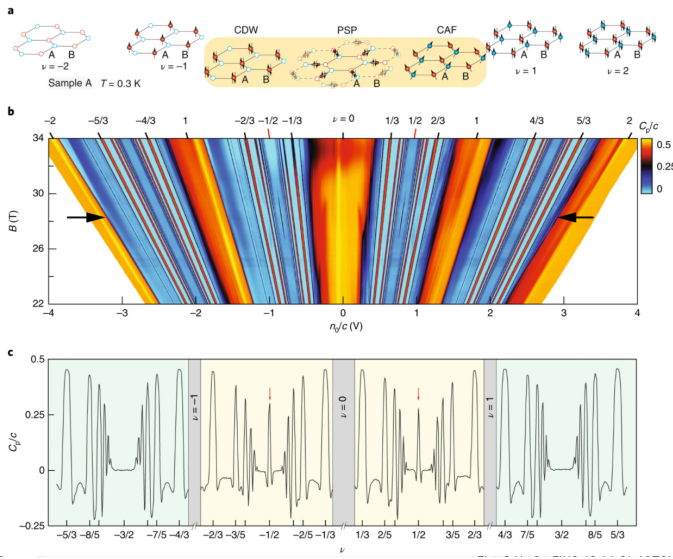


FIG. 1 (color online). Phase diagram for $SU(4)$ quantum Hall ferromagnetism in the $n = 0$ and $n = 1$ Landau levels of graphene. In our model the ordered region is bounded by a maximum value of ν_s , the ratio of the density of Coulomb scatterers to the density of a full Landau level. ν_s is inversely proportional to the product of the sample mobility and the external field strength and order near integer filling factors requires the minimum values for this product indicated on the right-hand vertical axis.



from: Nomura and MacDonald, Phys. Rev. Lett. 96, 256602 (2006); G. L. Yu et al., Nature Physics 10, 525-529 (2014)

Fractional Quantum Hall states at high B field

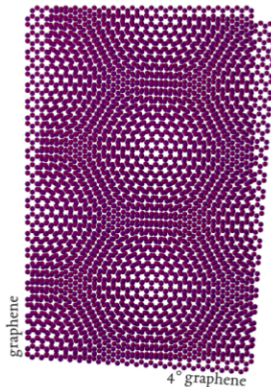


from: Zibrov et al., Nature Physics 14, 930-935 (2018)

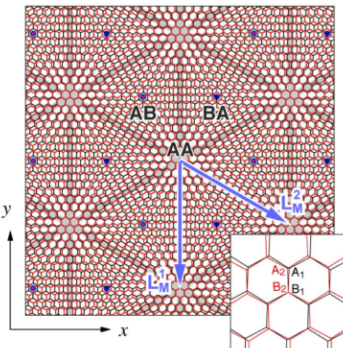
This page intentionally left blank

Correlated states in magic-angle moiré graphene

Flat bands in moiré graphene



Source: Wikipedia

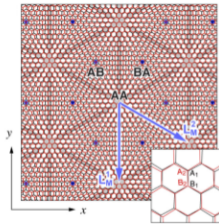
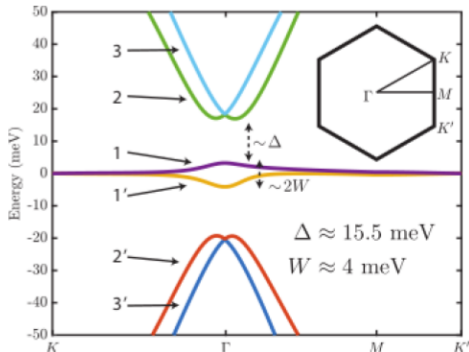


M. Koshino, et. al., Phys. Rev. X 8, 031087 (2018)

Correlated states in magic-angle moiré graphene

Flat bands in moiré graphene

- Extremely narrow bands at “magic” twist angle $\theta \sim 1^\circ$
- Narrow bandwidth, low Fermi velocity, $v_F/v_{F,0} \sim 1/100$

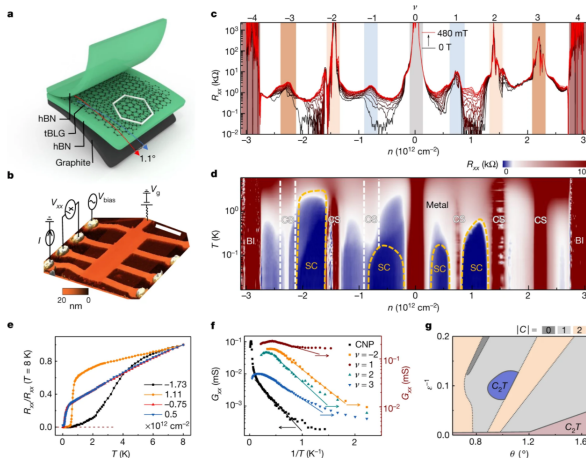


M. Koshino, et. al., Phys. Rev. X 8, 031087 (2018)

Correlated states in magic-angle moiré graphene

Mott-insulating states at band fillings $\nu = 0, \pm 1, \pm 2, \pm 3$; superconducting states in between (resembling high- T_c SC)

From: Superconductors, orbital magnets and correlated states in magic-angle bilayer graphene

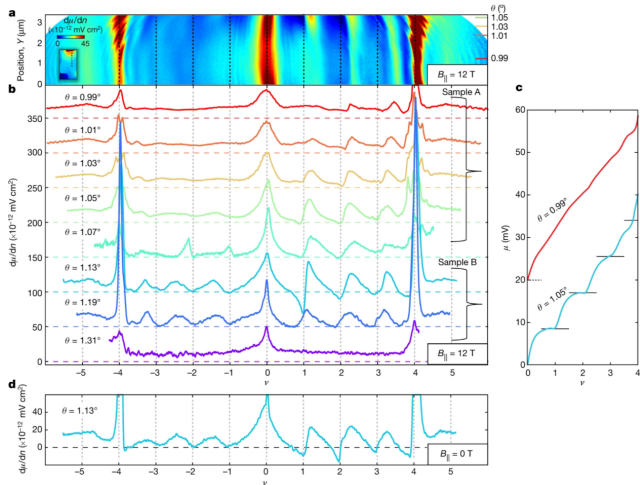


a. Schematic of a typical MAG device. **b.** Atomic force microscopy image and schematic of how various measurements are obtained. Scale bar, 2 μm . **c.** Four-terminal longitudinal resistance plotted against carrier density at different perpendicular magnetic fields from 0 T (black trace) to 480 mT (red

Correlated states in magic-angle moiré graphene

Stoner instability and Dirac resetting/revival transitions

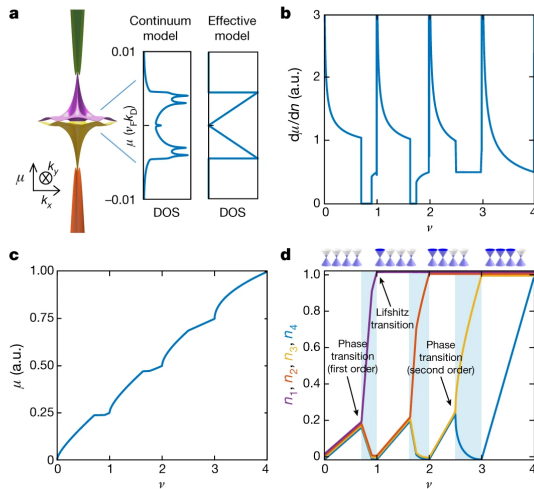
From: Cascade of phase transitions and Dirac revivals in magic-angle graphene



Correlated states in magic-angle moiré graphene

Stoner instability and Dirac resetting/revival transitions

From: Cascade of phase transitions and Dirac revivals in magic-angle graphene



Dynamical correlations and scattering measurements

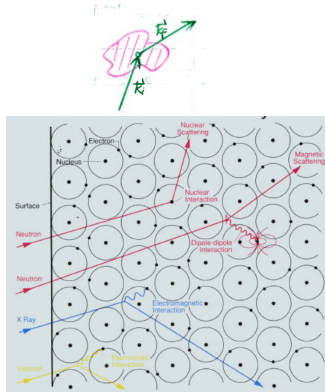
Dynamical (scattering) structure factor: general properties

Scattering measurements are widely used to probe microscopic dynamics at length scales of the order of the probe wavelength λ . In a typical setup, a beam of neutrons, x-rays or electrons of wavevector k_i is incident upon the sample and the scattered intensity is measured at wavevector $k_f = k_i + Q$. Most probes actually do not take a snapshot of the system, but look at time-averaged scattering. The observed scattering intensity is therefore proportional to an ensemble-averaged quantity — the dynamical correlation function of the density of particles in question:

$$S(Q, \omega) = \int dt e^{i\omega t} \langle \rho_Q(t) \rho_{-Q}(0) \rangle_T, \text{ with } \hbar Q \text{ and } \hbar \omega \text{ the momentum and energy transfer.}$$

The **dynamical structure factor** $S(Q, \omega)$ is defined through the pair correlation function of particle density $S(x, t) = \langle \phi_0 | \rho_H(x, t) \rho_H(0, 0) | \phi_0 \rangle$ where $\rho(x, t) = \sum_i \delta(x - x_i(t))$ (1st quantization), or

$$\rho(x, t) = \psi^\dagger(x, t) \psi(x, t) = \sum_{p, p'} e^{i(p-p')x - i(\epsilon_p - \epsilon_{p'})t} c_{p'}^\dagger c_p \quad (2\text{nd quantization})$$



Correlation functions and the dynamical structure factor

<u>Theory</u>		<u>Observable</u>
<i>Time correlation function</i>	\leftrightarrow	<i>Structure factor</i>
$\langle \rho(t + t_0) \cdot \rho(t) \rangle$	\leftrightarrow	$S(q, \omega)$
$S(q, \omega) = \frac{1}{N} \int_{-\infty}^{\infty} e^{i\omega t} \langle \rho(q, 0) \cdot \rho(-q, t) \rangle dt$ momentum energy $\rho(q, t) = \sum_i b_i \exp(-iq(t)r(t))$		

- * Why do theorists love it. A characteristic of system dynamics in the ground state. Immediate connection to linear response.
- * Why do experimentalists love it. Directly measurable (by scattering experiments), very informative

Dynamical structure factor: the detailed balance relation

Introducing particle density Fourier harmonics

$$\rho_{\mathbf{q}} = \int d^3x e^{-i\mathbf{q}\cdot\mathbf{x}} \rho(\mathbf{x}) = \begin{cases} \sum_j e^{-i\mathbf{q}\cdot\mathbf{x}_j} & \text{(1st quantization)} \\ \sum_{\mathbf{p}} c_{\mathbf{p}+\mathbf{q}}^\dagger c_{\mathbf{p}} & \text{(2nd quantization)} \end{cases}$$

(Note: $\rho_{-\mathbf{q}} = \rho_{\mathbf{q}}^\dagger$). Fourier transforming the correlation function $S(\mathbf{x}, t) = \langle \phi_0 | \rho_H(\mathbf{x}, t) \rho_H(0, 0) | \phi_0 \rangle$ in \mathbf{x} yields

$$S(\mathbf{q}, t) = \langle \phi_0 | \rho_H(\mathbf{q}, t) \rho_H(-\mathbf{q}, 0) | \phi_0 \rangle = \sum_n |\langle n | \rho_q^\dagger | 0 \rangle|^2 e^{-i(E_n - E_0)t}$$

Evaluate the dynamical structure factor $S(\mathbf{q}, \omega) = \int_{-\infty}^{\infty} e^{i\omega t} S(\mathbf{q}, t) dt$:

$$S(\mathbf{q}, \omega) = \sum_n |\langle n | \rho_q^\dagger | 0 \rangle|^2 \int dt e^{i(\omega - (E_n - E_0))t} = \sum_n |\langle n | \rho_q^\dagger | 0 \rangle|^2 2\pi\delta(\omega - (E_n - E_0))$$

Now, at a finite temperature $T > 0$, averaging as $\langle A \rangle_T = \frac{\text{tr}(e^{-\beta H} A)}{\text{tr}(e^{-\beta H})}$, by a similar argument find

$$S(\mathbf{q}, \omega) = \frac{1}{Z_0} \sum_{n,m} e^{-\beta E_m} |\langle n | \rho_q^\dagger | m \rangle|^2 2\pi\delta(\omega - (E_n - E_m))$$

Interchanging m and n yields a (fundamental and very general) “detailed balance” relation $S(-\mathbf{q}, -\omega) = e^{-\beta\omega} S(\mathbf{q}, \omega)$ [see it as a relation between the Stokes and anti-Stokes scattering components]

At $T = 0$, $S(\mathbf{q}, \omega) = 0$ for $\omega < 0$ (can't drain energy from ground state)

Dynamical structure factor: a relation to linear response

Compare $S(q, \omega)$ to the Kubo susceptibility $\rho_{q,\omega} = \chi(q, \omega)U_{q,\omega}$

$$\begin{aligned}\chi(q, \omega) &= \frac{i}{\hbar} \int_0^\infty dt e^{i\omega t} [\rho_q(t), \rho_{-q}(0)] \\ &= \sum_n \frac{\langle 0 | \rho_q | n \rangle \langle n | \rho_{-q} | 0 \rangle}{\omega - (E_n - E_0) + i\delta} - \frac{\langle 0 | \rho_{-q} | n \rangle \langle n | \rho_q | 0 \rangle}{\omega + (E_n - E_0) + i\delta}\end{aligned}$$

Then, $\chi''(q, \omega) = -\pi \sum_n |\langle n | \rho_q^\dagger | 0 \rangle|^2 \delta(\omega - (E_n - E_0))$

$-|\langle n | \rho_q | 0 \rangle|^2 \delta(\omega + (E_n - E_0))$ (Here we used $\frac{1}{x \pm i\delta} = P(\frac{1}{x}) \mp \pi i \delta(x)$).

This quantity is odd in ω : $\chi''(-q, -\omega) = -\chi''(q, \omega)$ as discussed above.
Previously we have identified $\chi''(\omega, q)$ and $\chi'(\omega, q)$ with the “dissipative”
and “reactive” parts of the response.

Linking $\chi''(q, \omega)$ and $S(q, \omega)$, we obtain an interesting/amazing relation

$$\chi''(q, \omega) = -\frac{1}{2}[S(q, \omega) - S(-q, -\omega)] \quad [\text{fluctuation - dissipation theorem}]$$

Now, at finite temperature, averaging as $\langle A \rangle_T = \frac{\text{tr}(e^{-\beta H} A)}{\text{tr}(e^{-\beta H})}$, by a similar argument find $\chi''(q, \omega) = \frac{1}{2}(e^{-\beta\omega} - 1)S(q, \omega)$.

For $T \rightarrow 0$, $\beta \rightarrow \infty$, we have $\chi''(q, \omega) = -\frac{1}{2}S(q, \omega)$ if $\omega > 0$, since $S(q, -\omega) = 0$ if $\omega > 0$ (can't drain energy from a ground state).

Or, inverting, $S(q, \omega) = -2(n_B + 1)\chi''(q, \omega)$, $n_B = \frac{1}{e^{\beta\omega} - 1}$.

Measuring the dynamical structure factor

To measure $S(q, \omega)$ perform scattering experiment, i.e. probe our system **dynamics** by scattering on it electrons, neutrons, photons, etc.

$$\mathcal{H}' = \sum_i V(x_i - R) = \sum_q \sum_i e^{iq(x_i - R)} V_q = \sum_q V_q \rho_q^\dagger e^{-iqR}$$

For electrons $V(x) = \frac{e^2}{|x|}$, $V_q = \frac{4\pi e^2}{q^2}$, for neutrons $V(x) = \frac{2\pi b}{M_n} \delta(x)$, etc.



Treating scattering as weak, we can use Born approximation (1st-order in V). From Fermi's Golden Rule, the transition rate is

$$P_{i \rightarrow f} = 2\pi \sum_f |\langle f | \mathcal{H}' | i \rangle|^2 \delta(E_f - E_i)$$

with the initial state $|i\rangle = |\phi_0\rangle \otimes |k_i\rangle$, where $|\phi_0\rangle$ is the system internal state and $|k_i\rangle$ the state of probe.

Define **momentum and energy transfer** $Q = k_i - k_f$, $\omega = \epsilon_{k_i} - \epsilon_{k_f}$.

Possible final states are $|n\rangle \otimes |k_f\rangle$, where n labels the microscopic eigenstates of the system, $E_n |n\rangle = H_0 |n\rangle$.

Focus on the probe degrees of freedom, integrate over R:

$$P_{k_i \rightarrow k_f} = 2\pi \sum_n \left| \sum_{q'} V_{q'} \langle n | \rho_{q'}^\dagger | 0 \rangle \int d^3R e^{-iq' R} e^{-ik_f R} e^{ik_i R} \right|^2 \delta(\omega - (E_n - E_0))$$

Evaluating $\int d^3R e^{-iq' R} e^{-ik_f R} e^{ik_i R} = (2\pi)^3 \delta(q' - Q)$, we have

$$P_{k_i \rightarrow k_f} = |V_Q|^2 2\pi \sum_n |\langle n | \rho_Q^\dagger | 0 \rangle|^2 \delta(\omega - (E_n - E_0))$$

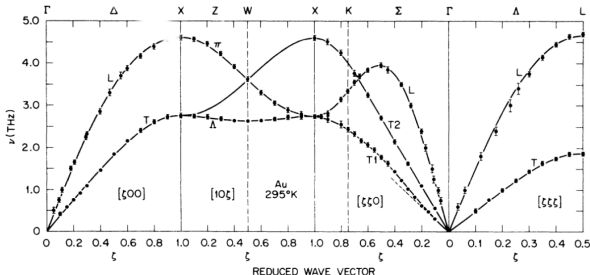
Identifying the RHS with $|V_Q|^2 S(Q, \omega)$ we express the scattering probability through the dynamical structure factor as

$$P_{k_i \rightarrow k_f} = |V_Q|^2 S(Q, \omega)$$

- * The resulting scattering crosssection depends on the probe through $|V_Q|^2$, and on system dynamics through the structure factor $S(Q, \omega)$.
- * Scattering probes collective excitations: phonons, spin waves, zero sound, plasmons, etc. (For a pedagogical derivation see [22.51 notes](#))
- * When the dynamical response function has poles, $\chi(q, \omega) \sim \frac{1}{\omega - \omega_0(q) + i\delta}$, the scattering crosssection with momentum transfer q features Stokes and anti-Stokes resonances at $\omega = \pm\omega_0(q)$, $q = Q$.

A tool of choice to probe the dispersion relation of elementary excitations
(phonons, spin waves, plasmons, etc)

Phonon dispersion relation in gold

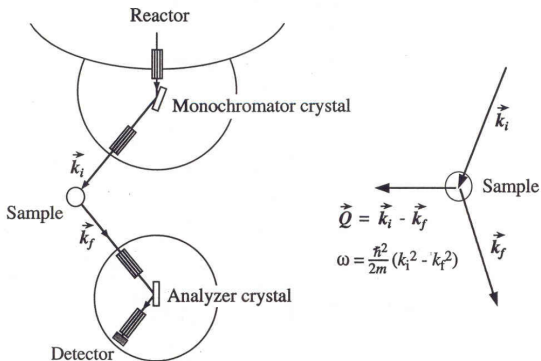


J. W. Lynn, H. G. Smith, and R. M. Nicklow, *Phys. Rev. B* **8**, 3493 (1973).

Measuring phonon dispersion can tell us about

- * interatomic potentials and bonding
- * structural phase transitions (soft modes)
- * many-body physics (e.g. electron-phonon coupling)

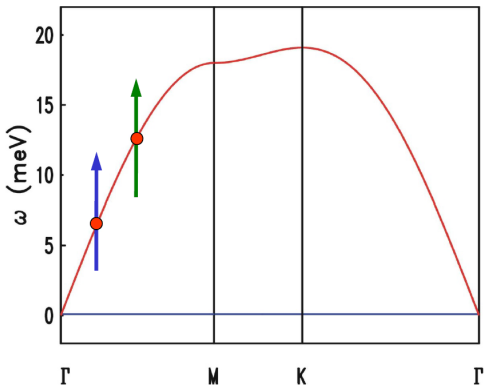
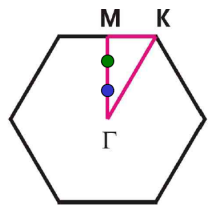
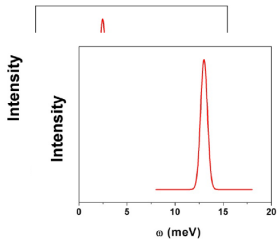
Triple-axis neutron scattering technique



Monochromator/analyzer crystals typically pyrolytic graphite (PG). Filters (also PG) are placed in beam to remove $\lambda/2$ neutrons.

Excitations of interest in solids: phonons and spin waves

Using neutrons to measure a dispersion surface

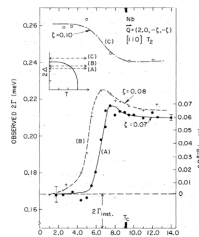
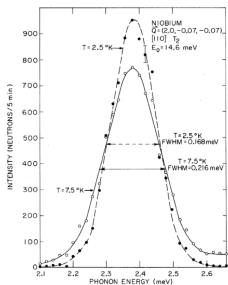


Example: Phonon lineshapes in conventional superconductors

Phonons in superconducting niobium crystals with neutron scattering at energies below the SC gap. **Question:** below T_c , do the phonon peaks become

- a) sharper, or
- b) broader?

Shapiro, et al, PRB 12, 4899 (1975)



The linewidth decreased below T_c (life-time increased), due to removal of decay channels with the metallic electrons which are gapped out.

Probing spin waves with neutron scattering

Spin Waves in 3d Metals*

G. SHIRANE, V. J. MINKIEWICZ, AND R. NATHANS
Brookhaven National Laboratory, Upton, New York

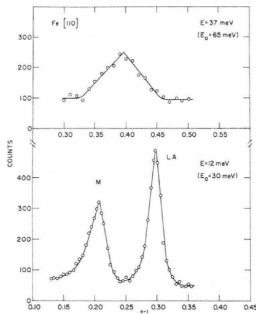


FIG. 2. Constant E scans of spin waves (M) and longitudinal acoustic (LA) phonons in Fe at 295 K with fixed incoming energy E_0 .

Triple-axis spectroscopy on single crystals

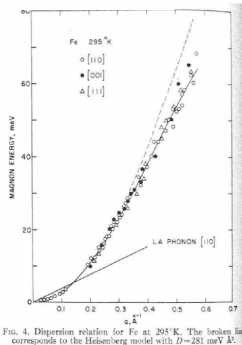


FIG. 4. Dispersion relation for Fe at 295 K. The broken line corresponds to the Heisenberg model with $D = 281 \text{ meV \AA}^2$.

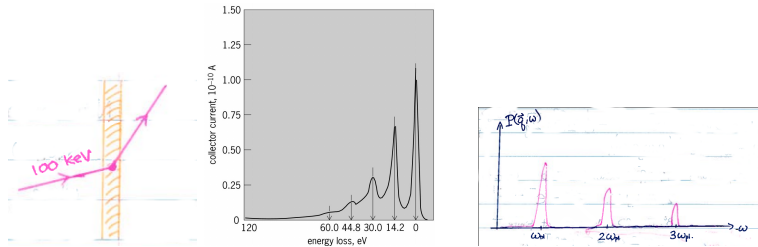
- quadratic dispersion (FM in iron)
- overlap with acoustic phonons

A wide variety of interesting examples for different types of magnetic order—see Young Lee's lectures

This page intentionally left blank

Scattering of fast electrons in thin metal films

It is instructive to revisit the problem of plasmon emission by fast electrons in metals, linking it to the general scattering theory formalism. We will show that the dynamical structure factor in this case is nothing but the loss function $\text{Im}[-1/\epsilon(Q, \omega)]$.



Number of detected electrons in a beam versus their energy loss during transit through a thin aluminum foil. (Electron number is expressed as a current; $10^{-14} A = 6.7 \times 10^6$ electrons per second.) Peaks at approximate multiples of 14.2 eV correspond to energy donated to plasmons in the aluminum. (After T. L. Ferrell, T. A. Calicott, and R. J. Warmack, Plasmons and surfaces, Amer. Sci., 73:344-353, 1985)

Plasmon resonances probed by electron scattering

Connect $S(Q, \omega)$ to the dielectric screening function $\epsilon(Q, \omega)$? We already know that the crosssection equals $P_{i \rightarrow f} \sim \left(\frac{4\pi e^2}{Q^2}\right)^2 S(Q, \omega)$. We therefore need the associated susceptibility defined as a density-potential response $\delta n = \chi(Q, \omega) U_{\text{ext}}$. Beware: here $\chi(Q, \omega) \neq \Pi(Q, \omega)$, defined through $\delta n = \Pi(Q, \omega) U_{\text{tot}}$! We show below that

$$\frac{1}{\epsilon(Q, \omega)} = 1 + \frac{4\pi e^2}{Q^2} \chi(Q, \omega) \quad (8)$$

Using the fluctuation-dissipation relation derived above,
 $S(Q, \omega) = -2\chi''(Q, \omega)$ (at low temperatures $1 - e^{-\beta\omega} \approx 1$) we can write

$$P_{i \rightarrow f} = \frac{4\pi e^2}{Q^2} 2 \operatorname{Im} \left(-\frac{1}{\epsilon(Q, \omega)} \right) \quad [\text{the loss function}]$$

To derive Eq.(8) we recall dielectric screening: $U_{\text{tot}} = U_{\text{ext}} + U_{\text{ind}}$,

$$\frac{1}{\epsilon(Q, \omega)} = \frac{U_{\text{tot}}(Q, \omega)}{U_{\text{ext}}(Q, \omega)} = 1 + \frac{U_{\text{ind}}(Q, \omega)}{U_{\text{ext}}(Q, \omega)}.$$
 Here the induced potential is related to the induced charge density through $-\nabla^2 U_{\text{ind}} = 4\pi e^2 \delta n_{\text{ind}}$, i.e.

$U_{\text{ind}}(Q, \omega) = \frac{4\pi e^2}{Q^2} \delta n(Q, \omega)$. Plasma approximation $\epsilon(\omega) = 1 - \frac{\omega_p^2}{\omega^2 + i\omega\tau}$,
 $\omega_p^2 \equiv \frac{4\pi e^2 n}{m}$, gives sharp resonances $S(Q, \omega) \sim \delta(\omega^2 - \omega_p^2)$ which is indeed what's seen in experiment.

Energy losses of fast charged particles in a solid

Here we recall the classical EM approach to describe energy losses of fast electrons transiting through a metal. The result is essentially equivalent to that found in our QM treatment above. Start with writing dissipated power as $P = E j_D = \frac{1}{4\pi} E \frac{\partial D}{\partial t}$. Plugging $E(t) = \text{Re } E_\omega e^{-i\omega t}$, $D(t) = \text{Re } \epsilon(\omega) E_\omega e^{-i\omega t}$ and averaging over fast oscillations gives the time-averaged dissipation rate $\langle P \rangle = \frac{1}{8\pi} \omega \epsilon''(\omega) E_\omega E_\omega^*$.

Next, the field of a moving particle, $x_0(t) = vt$, is $D = -\nabla \frac{e}{|x-x_0(t)|}$. Fourier transforming, first $x \rightarrow k$ and then $t \rightarrow \omega$, we get

$$D_{k,\omega} = \int dt e^{i\omega t} (-ik) \frac{4\pi e}{k^2} e^{-ikvt} = -ik \frac{4\pi e}{k^2} 2\pi \delta(\omega - kv).$$

Writing $E_{k,\omega} = \frac{1}{\epsilon(\omega)} D_{k,\omega}$ and plugging in our formula for dissipation gives

$$\langle P \rangle = \sum_{k,\omega} \frac{\omega \epsilon''(\omega)}{8\pi |\epsilon(\omega)|^2} \frac{(4\pi e)^2}{k^2} \delta(\omega - kv) = \sum_{k_\perp, \omega} \frac{\omega}{8\pi} \text{Im} \left(-\frac{1}{\epsilon(\omega)} \right) \frac{(4\pi)^2 e^2}{v(k_\perp^2 + \frac{\omega^2}{v^2})}$$

This result is true for any solid. It further simplifies for a metal, by

taking $\epsilon(\omega) = 1 - \frac{\omega_p^2}{\omega^2 + i\omega\gamma}$ and $\text{Im} \left(-\frac{1}{\epsilon(\omega)} \right) \approx \omega_p^2 \pi \text{sgn } \omega \delta(\omega^2 - \omega_p^2)$. In this case, the sum \sum_ω is dominated by $\omega = \pm\omega_p$, giving the angular distribution of emitted plasmons $\langle P \rangle \sim \frac{e^2}{v} \sum_{k_\perp} \frac{\omega_p^2}{k_\perp^2 + \omega_p^2/v^2}$ (see Kittel

The fluctuation-dissipation theorem will be further discussed as part of “Disordered electrons” topic